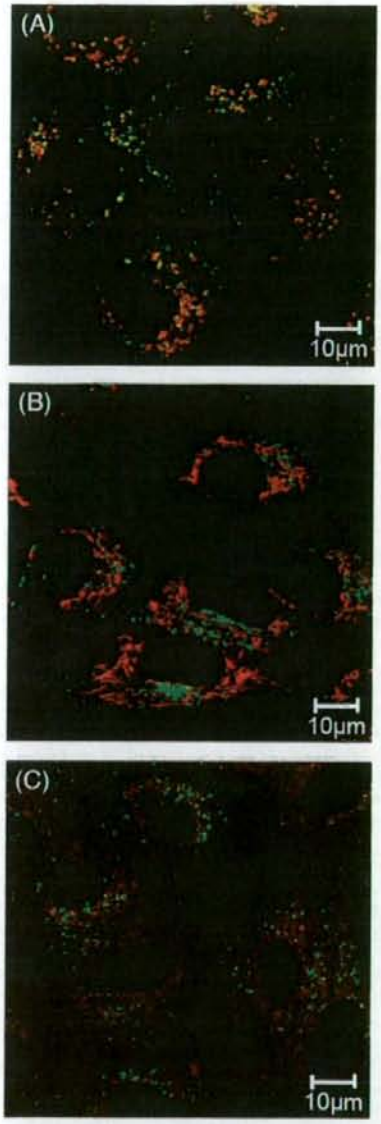

Fig. 3. Intracellular localization of Alexa488-labeled DPc/m (green) in A549 cells without photoirradiation. The cells were stained with LysoTracker Red DND-99 (red) for staining the lysosomes (A), MitoTracker Red 580 (red) for staining the mitochondria (B) and ER Tracker Red for staining endoplasmic reticulum (ER) (C).

PSs into nanocarriers generally decreases the singlet oxygen quantum yield due to the concentration quenching of PSs, leading to considerable reduction of photocytotoxicity [12,13]. In this study, we demonstrated that our unique photosensitizer–nanocarrier combination, i.e., dendrimer phthalocyanine (DPc)-encapsulated polymeric micelles (DPc/m), showed remarkably enhanced photocytotoxicity over free DPc, and achieved significantly higher *in vitro* and *in vivo* PDT effect compared with clinically used Photofrin® (PHE). Therefore, we also focused on the underlying mechanisms of the efficient photo-induced cell death by DPc/m.

In Table 1, DPc/m showed 78-fold higher photocytotoxicity than free DPc. Such remarkable enhancement of DPc/m's photocytotoxicity cannot be explained by the intracellular concentration of DPc: DPc/m exhibited only 7.6-fold higher cellular uptake than free DPc in A549 cells (data not shown). In addition, we previously demonstrated that DPc/m showed an approximately three- to fourfold slower oxygen consumption rate compared with free DPc [15]. We therefore assume that different mechanisms may underlie photo-induced cell death between DPc/m and free DPc. In the present paper, we also studied the effect of photoirradiation by a high-power diode laser on photocytotoxicity. As a result, there were considerable differences in the fluence-rate-dependency of photocytotoxicity between DPc and DP/m (Table 2). Meanwhile, we have also studied the time-dependent morphological changes of the cells during PDT, and found marked differences between DPc and DPc/m (Fig. 2). The DPc/m induced unprecedentedly rapid cell death accompanied by characteristic morphological changes including swelling and membrane blebbing. Note that such characteristic morphological changes in the DPc/m-treated cells appear to be similar to the characteristics of *oncosis*, which is reported to be induced by several pathological conditions, such as hypoxia, inhibition of ATP production, and increased permeability of the plasma membrane [23].

To further study unique light-induced cell death by DPc/m, we have studied intracellular localization of DPc/m. We observed that both DPc and DPc/m selectively accumulated in the endo-/lysosomes, suggesting their cellular internalization through the endocytosis (Fig. 3 and Fig. S2). However, once the cells were photoirradiated, the DPc and DPc/m may have been translocated from the endo-/lysosomes to the

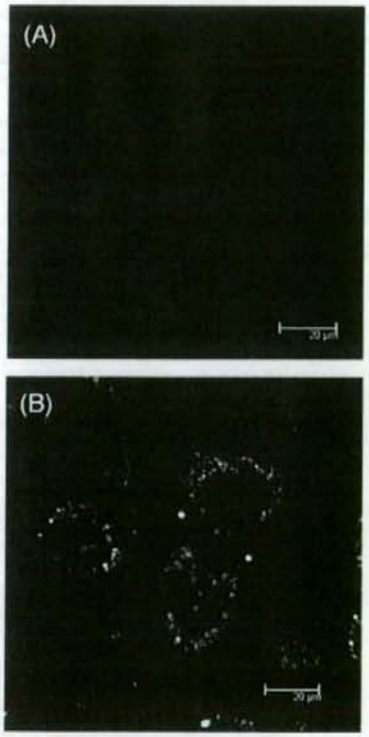

Fig. 4. Fluorescence of MitoSOX Red in the DPc- (A) and DPc/m (B)-treated A549 cells after 1 min photoirradiation.

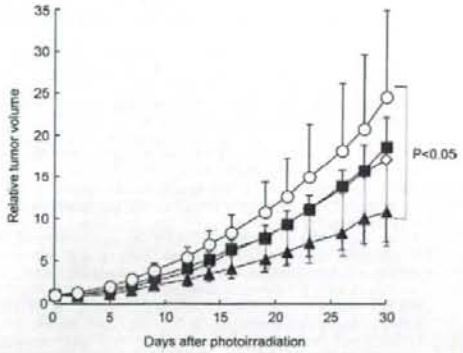

Fig. 5. Growth curves of subcutaneous A549 tumors in control mice (open circle) and mice administered with 0.37 μmol/kg DPc (closed square), 0.37 μmol/kg DPc/m (closed triangle) and 2.7 μmol/kg Photofrin® (PHE) (open diamond) ($n=6$). Twenty-four hours after administration of photosensitizing agents, the tumors were photoirradiated using a diode laser (fluence: 100 J/cm^2).

cytoplasm, because DPc fluorescence became apparent in a diffusive manner in both the DPc- and DPc/m-treated cells (Fig. 2). The mechanism of this translocation is the photochemical disruption of the endo-/lysosomal membranes: this is called photochemical internalization (PCI), a new concept for light-induced cytoplasmic delivery of cell-membrane-impermeable low-molecular-weight drugs as well as macromolecular compounds, such as nucleic acids and proteins [24,25]. In our previous papers, we indeed demonstrated that DPc and DPc/m allowed the efficient endosomal escape of non-viral gene vectors, achieving light-induced and site-directed transfection *in vitro* and *in vivo* [27,28]. Possibly, the increased fluorescence of DPc/m in Fig. 2 may reflect the destabilization of the micellar structure due to photochemical reactions: this destabilization may be essential to the interaction of DPc/m with the endo-/lysosomal membranes.

It is known that the efficiency of light-induced cell death in PDT depends on which sites in the cell are photodamaged [2,3]. In this regard, photodamage to the mitochondria could induce efficient cell death, whereas endo-/lysosomes are less susceptible to photocytotoxicity [3]. Therefore, we focused on the effects of PDT using DPc/m on the mitochondria. In Fig. 2, we evaluated the time-dependent changes in the fluorescence of Rh123, a specific dye to the mitochondria, during photoirradiation in PDT using DPc or DPc/m. The fluorescence of Rh123 in the DPc/m-treated cells immediately disappeared after the initiation of photoirradiation, whereas that in the DPc-treated cells remained even after 450 s photoirradiation. Note that the fluorescent intensity of Rh123 is correlated with the amount of ATP in the cells [28]. Therefore, it is assumed that DPc/m might directly or indirectly clip the ATP in the cell. To clarify whether the effects of DPc/m on the mitochondrial functions are attributed to its direct photodamage to the mitochondria or not, we detected the ROS production in the mitochondria by using MitoSOX Red (Fig. 4). As a result, only DPc/m showed appreciable ROS production in the mitochondria upon photoirradiation. These results suggest that DPc/m might induce photodamage to the mitochondria and thus affect their functions.

Based on all the aforementioned results, DPc and DPc/m are assumed to undergo the following steps in the photo-induced cell death. (i) DPc and DPc/m are internalized through the endocytic pathway and accumulate in the endo-/lysosomes. In this step, DPc/m showed 7.6-fold higher cellular uptake than free DPc. (ii) Upon photoirradiation, DPc and DPc/m are translocated from the endo-/lysosomes to the cytoplasm through the photochemical disruption of the endo-/lysosomal membranes. We previously reported that DPc/m is more efficient than DPc in the PCI-mediated gene transfection [26]. (iii) Only DPc/m might accumulate in the mitochondria and produce the ROS, resulting in exhaustion of ATP in the cell. In contrast, DPc showed no ROS production in the mitochondria. These steps may account for DPc/m's much higher photocytotoxicity compared to DPc. Also, PDT using DPc/m induced unique cell death, similar to a characteristic of *oncosis*. The photodamage to the mitochondria and/or the exhaustion of intracellular ATP may be attributed to this unique cell death by DPc/m. In addition to the subcellular localization of DPc/m and the photodamaged sites in the cell, the characteristic structure of DPc/m, in which several tens DPc molecules are concentrated in a 50 nm nanocontainer, may also contribute to the remarkably high photocytotoxicity. Note that DPc/m from PEG–PLL with the polymerization degree of PLL of 43 contained 77 DPc molecules in the core (Fig. S3 in Supporting Information). The high local concentration of DPc within the micellar core is assumed to generate a high concentration of ROS at a local site, achieving a high photochemical oxidation level that exceeds the threshold of cell death. Note that, in the case of other nanocarriers containing conventional PSs, it may be difficult to achieve such a high local concentration of ROS due to the concentration quenching of PSs [13]. Furthermore, although ROS, especially singlet oxygen, have very short half-lives (~2 μs) in aqueous media [3], a high local concentration of ROS achieved by DPc/m may allow the oxidization of the greater regions in the cell. Such effects of spatially regulated incorporation of PSs into nanocarriers on PDT are quite intriguing, and further studies should be performed.

In this study, we also demonstrated that DPc/m showed significantly higher *in vivo* antitumor activity against subcutaneous A549 tumors compared with clinically used PHE, although the injected dose of DPc/m was 7.3-fold lower than that of PHE on the basis of photosensitizing units (Fig. 5). This superior effect may be explained by the effective accumulation of DPc/m based on the EPR effect and its enhanced photocytotoxicity, as mentioned above. In general, *in vivo* PDT effect is known to be very complicated and can be affected by several parameters, including accumulation and penetrability of

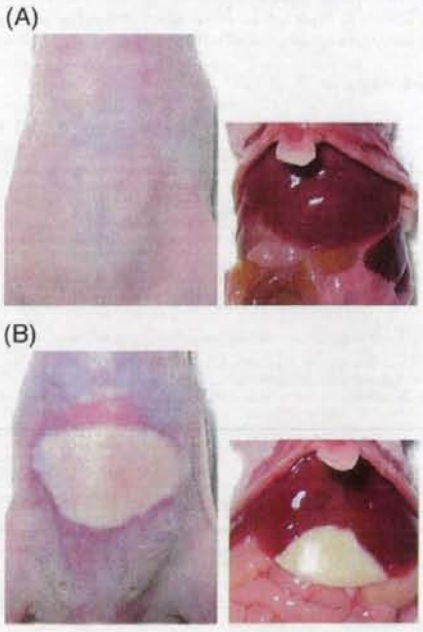

Fig. 6. Macroscopic observation of the skin and organs in the mice treated with 4.2 μmol/kg DPc/m (A) and 8.1 μmol/kg Photofrin® (PHE) (B) at 4 days after light irradiation to abdominal skin using a halogen lamp (fluence: 60 J/cm^2).

photosensitizers (PSs) in the tumor tissue, possible targets (i.e., tumor vasculature and cancer cells), and tissue penetration of light [1]; therefore, there may be a room for further improvement in the *in vivo* efficacy. In this regard, we are going to study the mechanism of *in vivo* PDT effect by DPc/m, optimizing several factors to maximize the therapeutic effect in the near future. Importantly, the PHE-administered mice showed severe damages to the skin and liver after exposure to white light; however, the DPc/m-administered mice did not show such side effects regardless of the injected dose (Fig. 6). These results may be attributed to the reduced accumulation of DPc/m in the skin and normal organs. In general, the skin phototoxicity might result from non-specific accumulation of conventional PSs in the skin, because they could penetrate the endothelium and eventually accumulate in various organs and tissues. In contrast, nanocarriers or macromolecular photosensitizers are assumed not to pass through the tight junctions of the vasculature in the tissues except for the liver, spleen, and tumor, which possess leaky vasculatures. Therefore, it is assumed that nanocarriers or macromolecular photosensitizers may not accumulate in the skin, thus preventing skin phototoxicity. Furthermore, no skin damage was found after photoirradiation even at 1 h after DPc/m administration (data not shown). Possibly, DPc/m in the bloodstream may not be photoactivated by light irradiation, owing to strong absorption by a heme in red blood cells.

5. Conclusion

The DPc/m elicited remarkably effective and rapid light-induced cell death. Following internalization by endocytosis, DPc/m seemed to be translocated from the endo-/lysosomes to the cytoplasm during photoirradiation and subsequently induce photodamage to the mitochondria. Such unique intracellular localization of DPc/m may be responsible for the enhanced photocytotoxicity mentioned above. In animal experiments, DPc/m showed significantly higher antitumor activity than clinically used PHE. Furthermore, unlike the PHE-treated mice, the DPc/m-treated mice showed no sign of skin phototoxicity. Thus, DPc/m is expected to serve as an innovative photosensitizer formulation to improve the effectiveness and safety of current PDT.

Acknowledgment

This study was supported by the New Energy and Industrial Technology Development Organization (NEDO) of Japan (project code: P06042).

Appendix A. Supplementary data

Supplementary data associated with this article can be found, in the online version, at doi:10.1016/j.jconrel.2008.10.010.

References

[1] D.E.J.G.J. Dolmans, D. Fukumura, R.K. Jain, Photodynamic therapy for cancer, Nat. Rev. Cancer 3 (5) (2003) 380–387.
[2] T.J. Dougherty, C.J. Gomer, B.W. Henderson, G. Jori, D. Kessel, M. Korbelik, J. Moan, Q. Peng, Photodynamic therapy, J. Natl. Cancer Inst. 90 (12) (1998) 889–905.
[3] I.J. Macdonald, T.J. Dougherty, Basic principles of photodynamic therapy, J. Porphyr. Phthalocyanines 5 (2) (2001) 105–129.
[4] A.S.L. Derycke, P.A.M. de Whitte, Liposomes for photodynamic therapy, Adv. Drug Deliv. Rev. 56 (1) (2004) 17–30.
[5] J.G. Shiah, Y. Sun, M. Peterson, R.C. Straight, J. Kopecek, Antitumor activity of N-(2-hydroxypropyl)methacrylamide copolymer-mesochlorine$_{e_6}$ and adriamycin conjugates in combination treatments, Clin. Cancer Res. 6 (3) (2000) 1008–1015.
[6] M.R. Hamblin, J.L. Miller, I. Rizvi, B. Ortel, E.V. Maytin, T. Hasan, Pegylation of a chlorine6 polymer conjugate increases tumor targeting of photosensitizer, Cancer Res. 61 (19) (2001) 7155–7162.
[7] C. Kojima, Y. Toi, A. Harada, K. Kono, Preparation of poly(ethylene glycol)-attached dendrimers encapsulating photosensitizers for application to photodynamic therapy, Bioconjug. Chem. 18 (3) (2007) 663–670.
[8] C.F. van Nostrum, Polymeric micelles to deliver photosensitizers for photodynamic therapy, Adv. Drug Deliv. Rev. 56 (1) (2004) 9–16.
[9] D. Le Garrec, J. Taillefer, J.E. Van Lier, V. Lenaerts, J.-C. Leroux, Optimizing pH-responsive polymeric micelles for drug delivery in a cancer photodynamic therapy model, J. Drug Target. 10 (5) (2002) 429–437.
[10] H.R. Stapert, N. Nishiyama, D.L. Jiang, T. Aida, K. Kataoka, Polyion complex micelles encapsulating light-harvesting ionic dendrimer zinc porphyrins, Langmuir 16 (21) (2000) 8182–8188.
[11] Y. Matsumura, H. Maeda, A new concept for macromolecular therapeutics in cancer chemotherapy: mechanism of tumoritropic accumulation of proteins and the antitumor agent SMANCS, Cancer Res. 46 (12) (1986) 6387–6392.
[12] N. Cauchon, H. Tian, R. Langlois, C. La Madeleine, S. Martin, H. Ali, D. Hunting, J.E. van Lier, Structure-photodynamic activity relationships of substituted zinc trisulfophthalocyanines, Bioconjug. Chem. 16 (1) (2005) 80–89.
[13] Y. Li, W.-D. Jang, N. Nishiyama, A. Kishimura, S. Kawauchi, Y. Morimoto, S. Miake, T. Yamashita, M. Kikuchi, T. Aida, K. Kataoka, Dendrimer generation effects on photodynamic efficacy of dendrimer porphyrins and dendrimer-loaded supramolecular nanocarriers, Chem. Mater. 19 (23) (2007) 5557–5562.
[14] N. Nishiyama, H.R. Stapert, G.D. Zhang, D. Takasu, D.L. Jiang, T. Nagano, T. Aida, K. Kataoka, Light-harvesting ionic dendrimer porphyrins as new photosensitizers for photodynamic therapy, Bioconjug. Chem. 14 (1) (2003) 58–66.
[15] W.-D. Jang, Y. Nakagishi, N. Nishiyama, S. Kawauchi, Y. Morimoto, M. Kikuchi, K. Kataoka, Polyion complex micelle for photodynamic therapy: incorporation of dendritic photosensitizer excitable at long wavelength relevant to improved tissue-penetrating property, J. Control. Release 113 (1) (2006) 73–79.
[16] W.-D. Jang, N. Nishiyama, G.D. Zhang, A. Harada, D.-L. Jiang, S. Kawauci, Y. Morimoto, M. Kikuchi, H. Koyama, T. Aida, K. Kataoka, Supramolecular nanocarrier of anionic dendrimer porphyrins with cationic block copolymers modified with polyethylene glycol to enhance intracellular photodynamic efficacy, Angew. Chem., Int. Ed. 44 (3) (2005) 419–423.
[17] N. Nishiyama, S. Okazaki, H. Cabral, M. Miyamoto, Y. Kato, Y. Sugiyama, K. Nishio, Y. Matsumura, K. Kataoka, Novel cisplatin-incorporated polymeric micelles can eradicate solid tumors in mice, Cancer Res. 63 (24) (2003) 8977–8983.
[18] K. Kataoka, A. Harada, Y. Nagasaki, Block copolymer micelles for drug delivery: design, characterization and biological significance, Adv. Drug Deliv. Rev. 47 (1) (2001) 113–131.
[19] N. Nishiyama, K. Kataoka, Current state, achievements, and future prospects of polymeric micelles as nanocarriers for drug and gene delivery, Pharmacol. Ther. 112 (3) (2006) 630–648.
[20] R. Ideta, F. Tasaka, W.-D. Jang, N. Nishiyama, G.-D. Zhang, A. Harada, Y. Yanagi, Y. Tamaki, T. Aida, K. Kataoka, Nanotechnology-based photodynamic therapy for neovascular disease using a supramolecular nanocarrier loaded with a dendritic photosensitizer, Nano Lett. 5 (12) (2005) 2426–2431.
[21] Z. Sheng, X. Ye, Z. Zheng, S. Yu, D.K.P. Ng, T. Ngai, C. Wu, Transient absorption and fluorescence studies of disstacking phthalocyanine by poly(ethylene oxide), Macromolecules 35 (9) (2002) 3681–3685.
[22] A. Harada, K. Kataoka, Formation of polyion complex micelles in an aqueous milieu from a pair of oppositely-charged block copolymers with poly(ethylene glycol) segments, Macromolecules 28 (15) (1995) 5294–5299.
[23] G. Majno, I. Joris, Apoptosis, oncosis, and necrosis. An overview of cell death, Am. J. Phathol. 146 (1) (1995) 3–15.
[24] K. Berg, P.K. Selbo, L. Prasmickaite, T.E. Tjelle, K. Sandvig, J. Moan, G. Gaudernack, O. Fodstad, S. Kjolsrud, H. Anholt, G.H. Rodal, S.K. Rodal, A. Hogset, Photochemical internalization: a novel technology for delivery of macromolecules into cytosol, Cancer Res. 59 (6) (1999) 1180–1183.
[25] A. Hogset, L. Prasmickaite, P.K. Selbo, M. Hellum, B.O. Engesaeter, A. Bonsted, K. Berg, Photochemical internalization in drug and gene delivery, Adv. Drug Deliv. Rev. 56 (1) (2004) 95–115.
[26] N. Nishiyama, Arnida, W.-D. Jang, K. Date, K. Miyata, K. Kataoka, Photochemical enhancement of transgene expression by polymeric micelles incorporating plasmid DNA and dendrimer-based photosensitizer, J. Drug Target. 14 (6) (2006) 413–424.
[27] N. Nishiyama, A. Iriyama, W.D. Jang, K. Miyata, K. Itaka, Y. Inoue, H. Takahashi, Y. Yanagi, Y. Tamaki, H. Koyama, K. Kataoka, Light-induced gene transfer from packaged DNA enveloped in a dendrimeric photosensitizer, Nature Mater. 4 (12) (2005) 934–941.
[28] C.S. Downes, M.J. Ord, A.M. Mullinger, A.R. Collinsm, R.T. Johnson, Novobiocin inhibition of DNA excision repair may occur through effects on mitochondrial structure and ATP metabolism, not on repair topoisomerases, Carcinogenesis 6 (9) (1985) 1343–1352.

Pharmaceutical Research, Vol. 26, No. 1, January 2009 (© 2008)
DOI: 10.1007/s11095-008-9712-2

Research Paper

A Photo-Activated Targeting Chemotherapy Using Glutathione Sensitive Camptothecin-Loaded Polymeric Micelles

Horacio Cabral,[2] Masataka Nakanishi,[1] Michiaki Kumagai,[2] Woo-Dong Jang,[4] Nobuhiro Nishiyama,[2,3] and Kazunori Kataoka[1,2,3,5]

Received June 21, 2008; accepted August 14, 2008; published online August 30, 2008

Purpose. A novel photo-activated targeted chemotherapy was developed by photochemical internalization (PCI) of glutathione-sensitive polymeric micelles incorporating camptothecin (CPT) prepared from thiolated CPT (CPT-DP) and thiolated poly(ethylene glycol)-*b*-poly(glutamic acid) (PEG-*b*-P(Glu-DP))
Methods. PEG-b-P(Glu-DP) and CPT-DP were synthesized and characterized by ^{1}H-NMR and gel permeation chromatography, and then mixed to prepare CPT-loaded polymeric micelles (CPT/m). The CPT release from the micelle was studied by reverse phase liquid chromatography. The PCI-activated cytotoxicity of CPT/m against HeLa cells was studied in combination with a non-toxic concentration of dendrimer phthalocyanine-loaded micelles (DPc/m) as the photosensitizer.
Results. The diameter of CPT/m was 96 nm and the drug loading was 20% (*w/w*). CPT was slowly released under the conditions reproducing the extracellular or endosomal environments. However, under the reductive conditions mimicking the cytosol, CPT was rapidly released achieving approximately 90% of the drug release after 24 h. The cytotoxicity of CPT/m was drastically increased on photoirradiation, whereas the CPT/m were not cytotoxic without PCI.
Conclusions. The CPT/m released the drug responding to reductive conditions. The PCI-induced endosomal escape exposed CPT/m to the cytosol triggering the drug release. Thus, CPT/m in combination with DPc/m will behave as smart nanocarriers activated only at photoirradiated tissues.

KEY WORDS: camptothecin; chemotherapy; environment sensitive-polymeric micelles; photochemical internalization.

INTRODUCTION

The site-specific drug delivery has become a key issue in cancer therapy, as the use of chemotherapeutic agents is often limited due to severe side effects, and the development of stimuli-responsive drug delivery systems that allow selective activation of the drugs at the target site will be crucial for successful therapies. In this way, the use of light for the activation of drug carriers is an attractive strategy because it is a safe energy source and it offers a high level of control in terms of wavelength, duration, intensity, and site of the photoirradiation, which can modulate the quantity of drug released, the timing of the release event and its location. The existing photoactivated drug delivery systems are mainly triggered by UV light, such as the systems based on the photoisomerization of azobenzene derivatives (1–5). Nevertheless, these systems are not suitable for biological applications because of the high absorbance of UV light by many biomolecules and the potential damage healthy tissues. Thus, it is necessary to develop realistic drug delivery systems activated by light with a longer wavelength in order to minimize photoinduced damage and to increase the depth of light penetration into tissues.

Recently, several macromolecules and other molecules that do not readily penetrate the plasma membrane have been used in combination with photochemical internalization (PCI) for the site-specific enhancement of their therapeutic efficacy by selective photochemical rupture of endocytic vesicles and consequent release of endocytosed macromolecules into the cytosol (6–13). The PCI concept is based on the

Electronic supplementary material The online version of this article (doi:10.1007/s11095-008-9712-2) contains supplementary material, which is available to authorized users.

[1] Department of Materials Engineering, Graduate School of Engineering, The University of Tokyo, 7-3-1 Hongo, Bunkyo-ku, Tokyo 113-8656, Japan.
[2] Center for Disease Biology and Integrative Medicine, Graduate School of Medicine, The University of Tokyo, 7-3-1 Hongo, Bunkyo-ku, Tokyo 113-0033, Japan.
[3] Center for NanoBio Integration, The University of Tokyo, 7-3-1 Hongo, Bunkyo-ku, Tokyo 113-8656, Japan.
[4] Department of Chemistry, College of Science, Yonsei University, Seoul, South Korea.
[5] To whom correspondence should be addressed. (e-mail: kataoka@bmw.t.u-tokyo.ac.jp)

ABBREVIATIONS: CPT, camptothecin; CPT-DP, thiolated CPT; PEG-*b*-P(Glu-DP), thiolated poly(ethylene glycol)-*b*-poly(glutamic acid); CPT/m, CPT-loaded polymeric micelles; DLS, dynamic light scattering; DPc/m, dendrimer phthalocyanine-loaded micelles; PCI, photochemical internalization; PDT, photodynamic therapy; PS, photosensitizer; SPTDP, disulfide amine linker; RPLC, reverse phase liquid chromatography.

0724-8741/09/0100-0082/0 © 2008 Springer Science + Business Media, LLC

use of photosensitizers, which induce the formation of reactive oxygen upon exposure to light of appropriate wavelengths (14). These photochemical reactions are the basis for photodynamic therapy (PDT), a treatment modality where light exposure leads to photosensitizer-induced killing of cancer cells used in various types of cancer (15,16). The PCI allows macromolecules located in the vesicles to reach the cytosol and to exert their biological activity instead of being degraded by lysosomal hydrolases. Furthermore, this PCI-based relocalization and activation of the macromolecules has the advantage of minimal side effects because the effect is localized to the irradiated area. The PCI employs light with clinically relevant wavelengths even in the near IR region, allowing a therapeutic effect in deeper lesions of the target tissues and a negligible damage to healthy tissue. In addition, after PCI, the macromolecules are exposed to the extremely reductive environment of the cytosol. Since the concentration of glutathione at the cytosol is 100–1,000 times higher than that in blood (17), it can be used as an efficient stimulus for the specific drug carrier activation. Consequently, the combination of PCI and drug carriers responsive to reductive environment will present the spatial and temporal triggering of drug action by photoirradiation.

The PCI-induced chemotherapy should be performed utilizing drug carriers that selectively accumulate in tumor tissues and enter cells *via* endocytosis. In this way, the polymeric micelles have shown reduced non-specific accumulation in normal tissues and preferential accumulation in solid tumors by the enhanced permeability and retention effect (18–22). Previously, we have reported polymeric micelles for the delivery of chemotherapeutics and photosensitizing agents with enhanced activity both *in vitro* and *in vivo* (11–13,18,20,23,24). Moreover, we have utilized dendrimer phthalocyanine (DPc)-loaded polymeric micelles (DPc/m), as photosensitizers, to increase the transfection efficiency of polyion complex micelles incorporating plasmid DNA by PCI (11–13). Thus, in the present study, we will utilize DPc/m to induce PCI for the specific activation of glutathione-sensitive camptothecin (CPT)-loaded polymeric micelles (CPT/m). Since both the CPT/m and the DPc/m are expected to exhibit prolonged blood circulation, selectively accumulate in tumor tissues and be taken up by cancer cells *via* endocytosis as previously reported for similar systems (18–21; Fig. 1), the combination will behave as a photoactivated drug delivery system for *in vivo* application.

CPT and its derivatives are very potent antitumor agents (25), though their full clinical potentials have yet to be realized because of the lack of water-solubility, the instability of the pharmacologically active lactone ring and the fast non-specific distribution to the whole body (25,26). Thus, the development of adequate carriers for the delivery of CPT is imperative. Herein, the CPT/m were prepared by conjugating a thiolated-camptothecin derivative (CPT-DP) to thiolated poly(ethylene glycol)-poly(glutamic acid) [PEG-*b*-P(Glu-DP)] block copolymer *via* a disulfide bond given that this bond is stable in blood and specifically cleaved in a reductive environment (17). Accordingly, the *in vitro* release profiles were studied under different conditions. Moreover, in order to prove the concept of a photoactivated drug delivery system, we tested the ability of CPT/m combined with a non-toxic concentration of DPc/m to specifically eradicate cancer cells *in vitro* after photoirradiation.

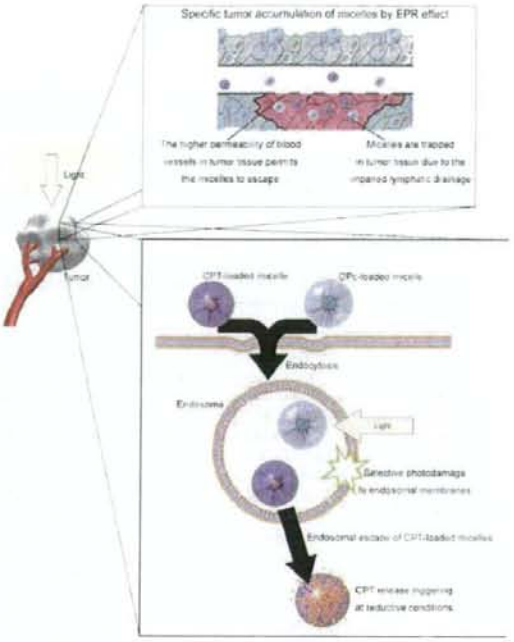

Fig. 1. Photochemical internalization-activated targeting chemotherapy. The polymeric micelles encapsulating camptothecin (*CPT*) and dendrimer phthalocyanine (*DPc*) accumulate in tumor tissue by the enhanced permeability and retention effect. The tumor is irradiated at the relevant wavelength. Both micelles are considered to be taken up by the cell through the endocytic pathway. The localization of the *DPc-loaded micelles* in the endosome allows the selective photodamage of the endosomal membrane upon photoirradiation, thereby inducing the endosomal escape of *CPT-loaded micelles* and the selective release of CPT under reductive conditions.

MATERIALS AND METHODS

Materials

γ-Benzyl L-glutamate and *N*-Z-L-lysine were bought from Sigma Chemical Co., Inc. (St. Louis, MO, USA). Bis(trichloromethyl)carbonate (triphosgene) was purchased from Tokyo Kasei Kogyo Co., Inc. (Tokyo, Japan). Dichloromethane, 4-dimethylaminopyridine (DMAP), dicyclohexylcarbodiimide (DCC), camptothecin, *N,N*-Dimethylformamide (DMF), dimethyl sulfoxide (DMSO), dithiothreitol (DTT) and 3-(4,5-dimethylthiazol-2-yl)-2,5-diphenyltetrazolium bromide (MTT) were obtained from Wako Pure Chemical Co., Inc. (Osaka, Japan). Methoxycarbonylsulfenyl chloride, 2-mercaptopyridine and 3-mercaptopropionic acid were purchased from Aldrich Chemical Co., Inc. (Milwaukee, WI, USA). α-Methoxy-ω-aminopoly(ethylene glycol) (CH_3O-PEG-NH_2; Mw=5,000 and 12,000) was purchased from Nippon Oil and Fats Co., Inc. (Tokyo, Japan). All solvents for the polymer syntheses were distilled just before use.

Cell Lines

Human cervical carcinoma HeLa cells were supplied from Japanese Collection of Research Bioresources Cell Bank (Osaka, Japan). HeLa cells were maintained in Dulbecco's Modified Eagle Medium (DMEM; Sigma Chemical Co., Inc.) containing 10% fetal bovine serum in a humidified atmosphere containing 5% CO_2 at 37°C.

Synthesis of Thiolated Camptothecin (CPT-DP)

A CPT derivative bearing the pyridyl disulfide group was synthesized as shown in Fig. 2. Briefly, a solution of methoxycarbonylsulfenyl chloride (1.25 g, 3.8 mmol) in methylene chloride (26 ml) was treated with 3-mercaptopropionic acid (1.05 g, 3.8 mmol) in methylene chloride (13 ml) for 2 h. After solvent was evaporated, the residue was redissolved in methylene chloride (26 ml) and treated dropwise with a solution of 2-mercaptopyridine (1.1 g, 3.8 ml) in 13 ml of the same solvent. After stirring overnight, the solvent was evaporated to yield an oily residue of 3-(2-pyrinyldithio)propionic acid. Then, 0.5 mmol of 3-(2-pyrinyldithio)propionic acid was mixed with 0.5 mmol CPT, 0.55 mmol DMAP and 0.55 mmol EDC in 5 ml methylene chloride. After 24 h stirring at room temperature, the mixture was diluted with 150 ml methylene chloride and washed with 0.01 N HCl (30 ml, one time) and water (30 ml, six times). The organic layer was evaporated to obtain a pale orange solid. The product was purified by silica gel chromatography using methylene chloride-methanol (97:3 *v/v*) as an eluent to yield an orange solid of CPT-DP. The proper modification of CPT was analyzed by ^{1}H-NMR in DMSO at 25°C

Synthesis of Thiolated Poly(ethylene glycol)-Poly(glutamic acid) [PEG-*b*-P(Glu-DP)] Block Copolymer

Preparation of Disulfide Amine Linker

Thiopyridyl disulfide was dissolved in 20 ml of methanol and 0.8 ml of acetic acid. Into this solution was added dropwise over a period of 0.5 h 2-aminoethylthiol hydrochloride in 10 ml methanol. The mixture was stirred for 48 h and then evaporated to yield yellow oil, followed by washing with 50 ml diethyl ether and dissolution in 10 ml of methanol. The product was precipitated by addition of 200 ml of diethyl ether, chilled for 12 h at −20°C and collected by vacuum filtration (yield: 77%).

Synthesis of Poly(ethylene glycol)-Poly(glutamic acid) [PEG-b-P(Glu)] Block Copolymer

PEG-P(Glu) block copolymer was synthesized according to the previously described synthetic method (27). Briefly, the *N*-carboxy anhydride of γ-benzyl L-glutamate (BLG-NCA) was synthesized by the Fuchs–Farthing method using triphosgene. Then, BLG-NCA was polymerized in DMF, initiated by the primary amino group of CH_3O-PEG-NH_2, to obtain PEG-poly (γ-benzyl L-glutamate) (PEG-b-PBLG) block copolymer. The molecular weight distribution of PEG-b-PBLG was determined by gel permeation chromatography [column: TSK-gel G3000HHR, G4000HHR (Tosoh Co., Inc., Yamaguchi, Japan); eluent: DMF containing 10 mM LiCl; flow rate—0.8 ml/min; detector: refractive index; temperature: 25°C]. The polymerization degree of PBLG was verified by comparing the proton ratios of the methylene units in PEG (–OCH_2CH_2–; δ= 3.7 ppm) and the phenyl groups of PBLG (–$CH_2C_6H_5$: δ= 7.3 ppm) in ^{1}H-NMR spectrum (solvent: DMSO-d_6; temperature: 80°C), and it was determined to be 81. The deprotection of the benzyl group of PEG-b-PBLG was carried out by mixing with 0.5 N NaOH at room temperature to obtain PEG-P(Glu).

Synthesis of Thiolated Poly(ethylene glycol)-b-Poly(glutamic acid) [PEG-b-P(Glu-DP)] Block Copolymer

The P(Glu) backbone of PEG-b-P(Glu) was thiolated by the procedure illustrated in the Fig. 3. Briefly, PEG-b-P (Glu) was dissolved in DMSO, followed by addition of NHS and water soluble DCC. The solution was stirred for 2 h, and

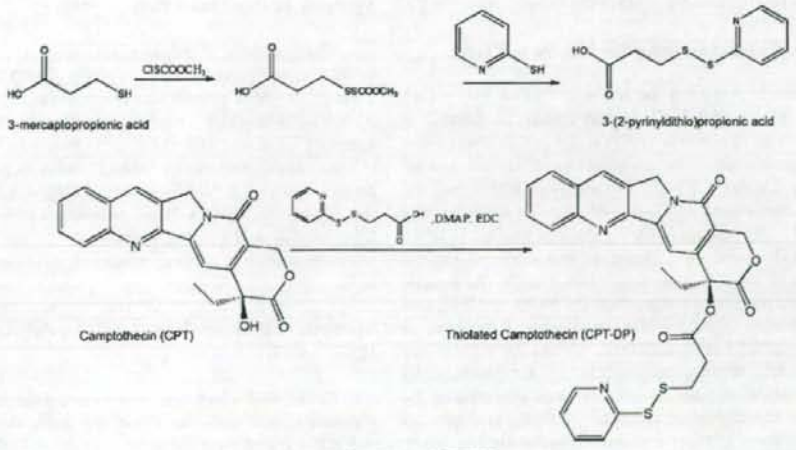

Fig. 2. Synthesis of CPT-DP.

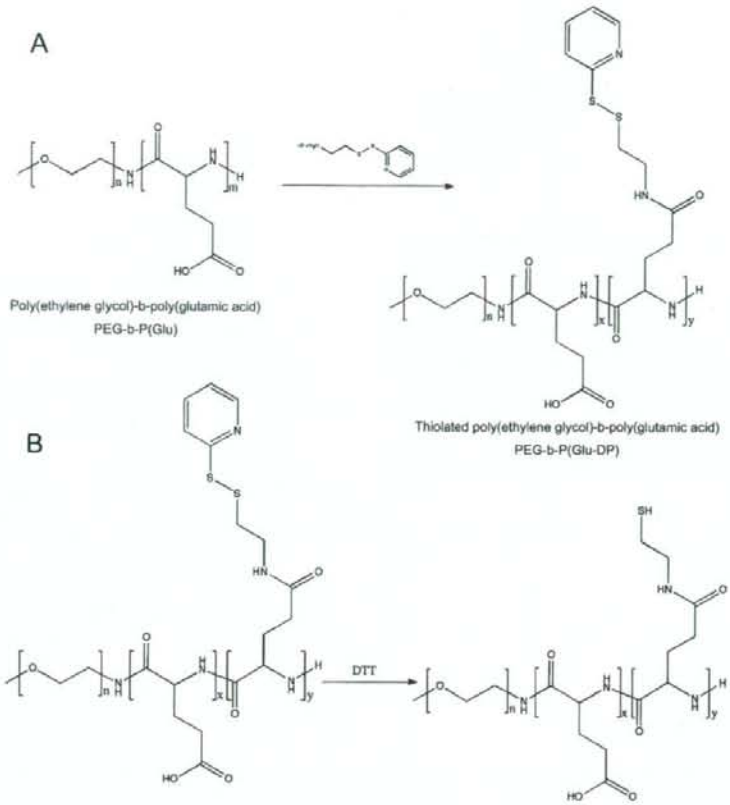

Fig. 3. **A** Synthesis of thiolated (PEG-*b*-P(Glu-DP) **B** Deprotection of PEG-*b*-P(Glu-DP) using DTT.

then SPTDP was added. The solution was stirred for another 20 h. Then, the mixture was dialyzed against water and finally freeze-dried. The characterization of the polymer was performed by ^{1}H-NMR (solvent: DMSO-d6; temperature: 80°C).

Preparation of Camptothecin-loaded Micelle (CPT/m)

CPT/m were prepared as follows: PEG-*b*-P(Glu-DP) (60 mg) was mixed with DTT (3-fold excess) in DMSO in order to deprotect the sulfide group at the *p*(Glu) backbone. Twenty-four hours later, the solution was dialyzed against DMSO. After dialysis, CPT-DP, (40 mg) was added and the solution was shaken at 37°C in dark for 72 h. Then, the unreacted CPT-DP was removed by dialysis against DMSO. The resulting drug-polymer conjugate was dialyzed against water in order to form polymeric micelles. Finally, the micelle solution was purified by ultrafiltration (MWCO—50,000) and the size distribution of the micelle was measured by dynamic light scattering (DLS) using a Zetasizer Nano ZS90 (Malvern Instruments Ltd., Worcestershire, United Kingdom). The CPT concentration of micelle solution was determined by reverse phase liquid chromatography (RPLC) [column: μ-Bondasphere (Waters, Japan); eluent: acetonitrile/1% acetic acid; detector: fluorescence (emission—370 nm; detection—440 nm); temperature: 40°C] after micelle dissociation with 10 mM DTT and mixing in 1 N HCl.

Synthesis of Dendrimer Phthalocyanine

The synthesis of the ionic DPc was performed according to the method reported by Ng's group (28). The second generation of dendritic phenol was reacted with 4-nitrophtalonitrile by an alkali-mediated coupling reaction to obtain the corresponding dendritic phthalonitrile, which was treated with Zn $(OAc)_2$ and 1,8-diazabicyclo[5.4.0]undec-7-ene (DBU) in *n*-pentanol to give DPc. The obtained DPc was 4,904 dalton and the adsorption spectra in an aqueous solution revealed that DPc exhibits a B band absorption at 350 nm and a strong Q band absorption at 685 nm, indicating a monomeric dispersion (24).

Synthesis of Poly(ethylene glycol)–*b*-poly(*l*-Lysine) [PEG-*b*-PLL]

PEG-*b*-PLL block copolymer was synthesized as previously reported (29). Briefly, the *N*-carboxy anhydride of *N*-Z-Lysine was polymerized from the ω-NH_2 group of CH_3O-PEG-NH_2 in DMF under Ar to obtain PEG-*b*-PLL(Z), followed by the

deprotection of the Z group. The polymerization degree of the PLL segments was determined to be 49 by ^{1}H-NMR.

Preparation of Dendrimer Phthalocyanine-loaded Micelle

The DPc/m was prepared as previously described (24). Briefly, DPc was dissolved in 10 mM Na_2HPO_4 (1 ml) and added to PEG-*b*-PLL in a 10 mM NaH_2PO_4 (0.457 ml) to give a solution containing DPc/m in 10 mM phosphate buffered solution (pH 7.4). The size distribution of DPc/m was determined by DLS.

CTP Release from CPT/m under Different Conditions

The release of CPT from the micelle under different conditions was evaluated by the dialysis method. Briefly, a micellar solution of known CPT concentration was placed inside a dialysis bag and dialyzed against 10 mM PBS plus 150 mM NaCl (pH 5 and 7.4) or 10 mM PBS plus 3 mM DTT at 37°C. The solution outside the dialysis bag was sampled at defined time periods to determine the amount of free CPT released from the micelle. Then, 0.1 ml of the sample was diluted in 0.4 ml of 1 N HCl, and the concentration was measured by RPLC using the conditions previously described.

In Vitro Photocytotoxicity of DPc/m

In order to determine the non-toxic concentration of DPc/m that will be used for the PCI of CPT/m, the growth-inhibitory activity of the DPc/m was evaluated by MTT assay. HeLa cells were cultured in DMEM containing 10% FBS in 96-well multiplate. After 24 h incubation, cells were incubated with the drugs for 24 h, followed by photoirradiation for 10 min using a 300 W halogen lamp (fluence rate: 3.0 mW cm^{-2}) equipped with a band-pass filter (400–700 nm). Then, the cells were post-incubated for 24 and 48 h. The cell viability was measured by MTT assay.

PCI-enhanced *In Vitro* Cytotoxicity of Camptothecin-loaded Micelle

The growth-inhibitory activity of the free CPT, free CPT-DP and CPT/m with and without a non-toxic concentration of DPc/m was evaluated by MTT assay. HeLa cells were cultured in DMEM containing 10% FBS in 96-well multiplate. After 24 h incubation, the cells were exposed to each CPT formulation in the combination with DPc/m. Twenty-four hours after drug exposure, the cells were photoirradiated 10 min. Then, the cells were post-incubated for 24 and 48 h. Finally, MTT solution was added and, 3 h later, 20% SDS solution was added. Cell viability was measured by the formed formazan absorbance at 570 nm.

RESULTS

CPT-loaded Micelle

The proper incorporation of the linkers to CPT and PEG-*b*-P(Glu) was confirmed by ^{1}H-NMR. After column purification, the spectra of CPT-DP presented the proton peaks corresponding to the CPT plus the alkyl-disulfide-pyridine linker (Fig. 4). From the proton ratio between the methylene group *j* of CPT (Fig. 4A) and the methylene protons, *1* or *2*, of the conjugated linker, the degree of modification of CPT was determined to be 100% by ^{1}H-NMR (Fig. 4B). Moreover, the RPLC results showed a single peak suggesting high purity of the product (Fig. 4C). For the PEG-*b*-P(Glu-DP), the degree

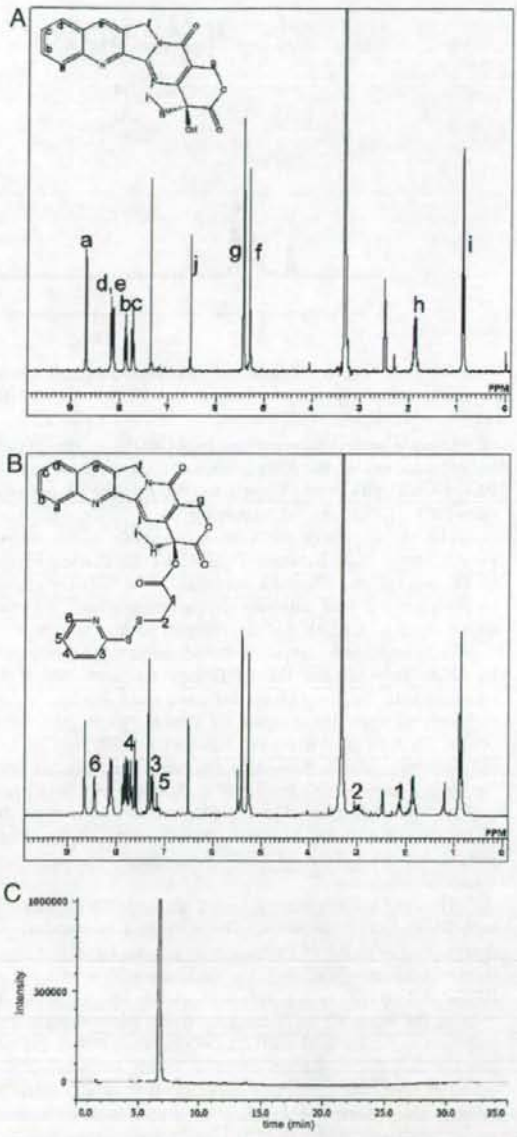

Fig. 4. Characterization of the thiolated camptothecin derivative. **A** ^{1}H-NMR spectra of CPT; **B** ^{1}H-NMR spectra of thiolated camptothecin (CPT-DP); **C** RPLC chromatogram of CPT-DP.

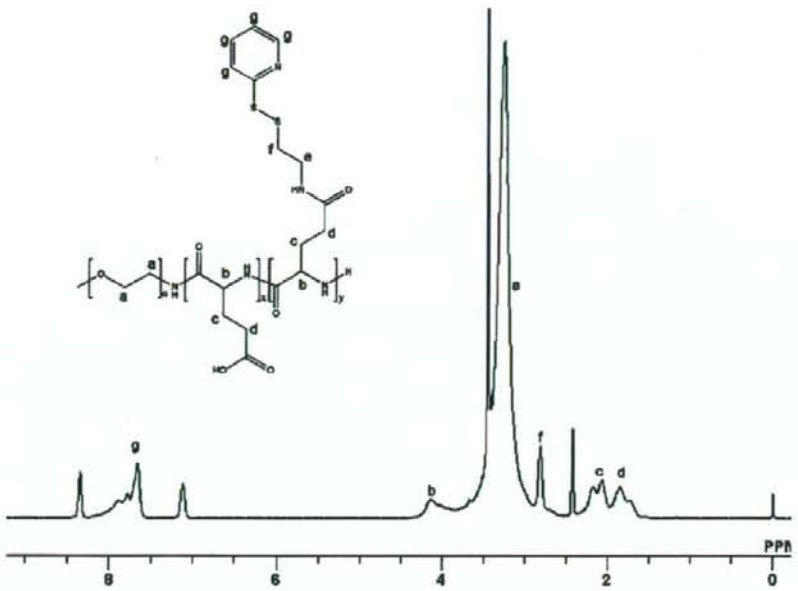

Fig. 5. ^{1}H-NMR spectra of thiolated poly(ethylene glycol)-poly(glutamic acid) block copolymer (PEG-*b*-P (Glu-DP)).

of thiolation was determined to be 44 [54% of the P(Glu) units] by comparing the proton ratios of the methylene units in PEG (–OCH_2CH_2–: δ=3.7 ppm) and the pyridine groups of P (Glu-DP) (–CH_5H_4N: δ=7.5 ppm; Fig. 5).

The driving force for micelle assembly is the hydrophobic interaction between P(Glu-DP) backbones of the block copolymers after the conjugation of CPT-DP. After purification of the micelles by ultrafiltration, the size distribution of CPT/m was determined to be 96.3 nm with a considerable low cumulant polydispersity (μ_2/Γ^2=0.048) by DLS. In addition, the CPT/m formulation offers the possibility to be lyophilized for long-term storage. After redissolving the freeze-dried CPT/m in water, the DLS results showed a z-average diameter of 100 nm and a polydispersity of 0.1. Note that the size of a colloidal drug carrier is a determinant feature of its fate in blood circulation and its biodistribution. The sub-100 nm size as well as the hydrophilic PEG palisade surrounding the core are important features of the CPT/m to avoid their uptake by the reticuloendothelial system.

The drug loading was estimated after micelle dissociation with 10 mM DTT by RPLC. The incorporated amount was determined to be 0.25 CPT molecules per thiol group at the p (Glu) backbone ([CPT-S]/[SH]), indicating 20% of CPT to PEG-*b*-P(Glu-DP) (*w*/*w*). This corresponds to approximately 35% of the initial CPT-DP feeding. Worth mentioning is that the thiol moieties in the P(Glu-DP) backbone that did not react with CPT may form disulfide bonds to crosslink the micellar core. We previously reported that similar micellar systems show complete disulfide bond formation by spontaneous oxidation of the thiol groups in the solution (30–32). Such disulfide crosslinks may stabilize the micelle structure in addition to the hydrophobic interaction.

Release Rate from CPT/m under Different Conditions

Drug-loaded micelles should be designed to release their contents after reaching the targeted tissue since the premature drug release can lead to toxic effects. Hence, the CPT release rate was studied under different conditions simulating different biological environments (Fig. 6). At settings that reproduce the extracellular environments, i.e. 10 mM phosphate buffer pH 7.4 plus 150 mM NaCl, the CPT release from the micelle was extremely low. After 96 h, the release was determined to be almost 30% of the incorporated CPT (Fig. 6). At endosomal pH, i.e. pH 5.5, the percentage of drug released from the micelle core was also found to be very low with approximately 1% of the drug released after 96 h (Fig. 6). Nevertheless, in a reductive environment simulating the cytosolic conditions, 10 mM PBS plus 3 mM DTT, a burst release of CPT was observed throughout the first 10 h. During this period, almost 80% of the incorporated drug was released. Then, the drug release reached a plateau achieving more than 90% of the drug released in 96 h (Fig. 6). This fast and preferential drug release under cytosolic conditions can be exploited to deliver CPT only in tissues where the micelles can escape from the endosomes aided by PCI.

In Vitro Photocytotoxicity of DPc/m

Hela cells were incubated with different concentrations of DPc/m for 24 h. Then, HeLa cells were photoirradiated at the fluence rate of 3.0 mW/cm^2 for 10 min (fluence—1.8 J/cm^2) and then post-incubated for 24 and 48 h. The results presented a DPc concentration-dependent decrease in cell viability (Fig. 7A and B). The photo-induced cell death is observed at the region of high DPc concentrations, and it

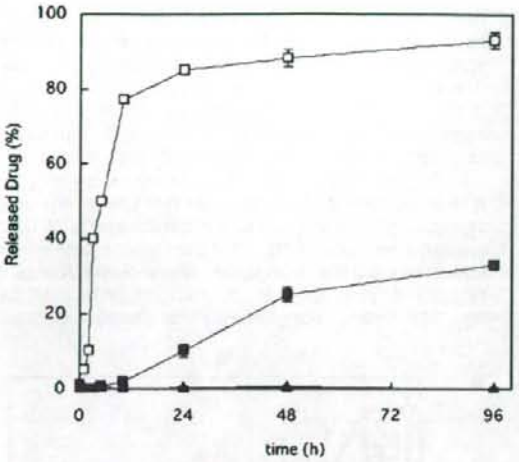

Fig. 6. Release rate of CPT-DP from the micelles (CPT/m) at 10 mM phosphate buffer plus 150 mM NaCl at pH 5.5 (*filled triangle*); pH 7.4 (*filled square*); and 3 mM DTT (*unfilled square*). Determined by RPLC (acetonitrile:1% acetic; fluorescence emission: 370 nm; fluorescence detection—440 nm). Data are shown as mean ± SD (n=3).

might be attributable to the vast photochemical reactions. At low DPc concentrations, the production of reactive oxygen species may be low and mainly confined to the endosomal compartments, maintaining the cell viability. Thus, in order to minimize the photocytoxicity from the DPc/m in the following PCI-mediated enhancement of CPT/m, a non-toxic concentration of DPc/m was determined. The highest non-toxic concentration of dendrimer-micelle was observed at 1×10^{-3} mg/ml. Therefore, the DPc/m concentration was fixed at 1×10^{-4} mg/ml for the following experiments.

PCI-Enhanced *In Vitro* Cytotoxicity of CPT/m

The cytotoxicity of free CPT, free CPT-DP and CPT/m in combination with the non-toxic concentration of DPc/m with and without photoirradiation against HeLa cells is shown in Figs. 8 and 9, and IC50 values are summarized in Table I. As shown in Fig. 8 and Table I, free CPT-DP showed slightly higher cytotoxicity than free CPT, which may be due to facilitated cellular uptake of CPT-DP with a hydrophobic pyridyl disulfide group. In the presence of photoirradiation, the combination of free CPT or CPT-DP and DPc/m showed less than 2-fold enhancement of the cytotoxicity without photoirradiation. Because free CPT or CPT-DP enter cells by passive diffusion and show potent cytotoxicity without photoirradiation, there may be a synergistic effect between cytotoxic compounds (i.e., fee CPT and CPT-DP) and photodynamic effect by DPc/m. This effect is assumed to be the combination effect of chemotherapy and PDT rather than PCI, since PCI is aimed to deliver cell membrane-impermeable drugs and macromolecular compounds from the endo-/lysosomes to the cytosol through the photochemical disruption of endo-/lysosomal membranes, thus achieving the light-selective drug action (9). On the other hand, the combination of CPT/m and DPc/m without photoirradiation was not toxic after 24 h post-incubation, probably due to the localization of the micelles in the endosome and the restricted drug release of CPT/m (Fig. 9A). However, when the cells were photoirradiated, the PCI effect exposed the CPT/m to the reductive conditions of the cytosol by endomal escape. Hence, the *in vitro* cytotoxicity of CPT/m was considerably increased (Fig. 9A), suggesting that the antitumor activity of CPT/m can be significantly enhanced by photoirradiation. At 48 h, the combination of CPT/m and DPc/m without photoirradiation slightly decreased the cell viability at high CPT/m concentrations (Fig. 9B). Nevertheless, the PCI using DPc/m significantly enhanced the antitumor activity of CPT/m at 48 h (Fig. 9B). Thus, as shown in Table I, the combination of CPT/m and DPc/m achieved remarkable (6.5-fold or much more) enhancement of the cytotoxiciy by photoirradiation.

DISCUSSION

Berg and Høgset *et al.* were the first to combine PCI and chemotherapy to deliberately increase the internalization of the anticancer drug bleomycin (33). The PCI-mediated relocalization of bleomycin into the cytosol considerably enhanced its *in vitro* and *in vivo* efficacy because bleomycin is practically non-permeant to the plasma membrane and enters the cells by endocytosis whereby it may be degraded in the lysosomes. Nevertheless, bleomycin is in contrast to traditional anticancer agents, such as CPT, that will easily pass the cell membrane and will generally be taken up by non-target cells generating severe side effects. Therefore, the PCI site-specific targeting of traditional anticancer drugs should be performed using drug carriers that enter the cells *via* endocytosis and release their contents only after PCI. In this way, the CPT/m presented a strong *in vitro* cytotoxicity after endosomal escape by PCI. The carrier activation is correlated with the fast CPT release from the micelle core under reductive conditions. Moreover, the modification of the outer hydrophilic shell of CPT/m with cancer-specific ligands can increase the specific uptake in tumor cells and the efficiency will be considerably enhanced.

The CPT/m were also designed to release their contents after reaching the targeted tissue. Like this, the drug leakage from CPT/m during blood circulation will be minimized since the experiments of drug release rate demonstrated that the disulfide linker used to conjugate CPT to the block copolymer backbone is selectively cleaved under reductive conditions. This will reduce the toxic effects that arise from non-specific accumulation of free drug. Moreover, the delivery of the active lactone form of CPT is also crucial for exerting the antitumor activity. In this way, it has been determined that modifying CPT at the 20 position as an ester stabilizes the active lactone ring under physiological conditions (34). Accordingly, the CPT instability under physiological conditions may also be reduced for the CPT-DP derivative. In addition, previous studies revealed that the lactone ring of CPT was protected upon incorporation of the drug into the lipid bilayer of liposomes (35,36), microspheres (37,38), nanobiohybrids (39), and polymeric micelles (40,41). Thus, the hydrophobic core of CPT/m probably functions as an auspicious CPT reservoir by inhibiting drug inactivation. In addition, after the PCI, the CPT/m will reach the interior of cancer cells, release the CPT in the lactone form avoiding extracellular inactivation and, in this way, maximize the efficiency of CPT.

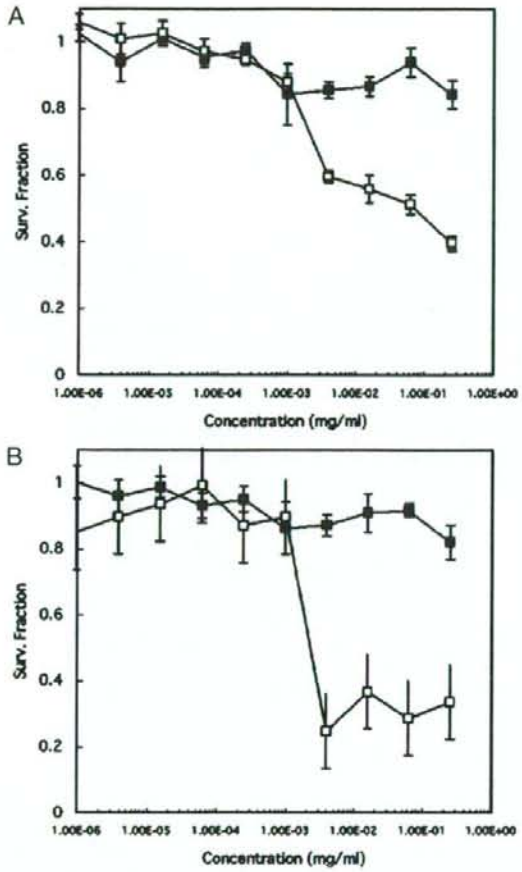

Fig. 7. Cell viability of dendrimer phthalocyanine-loaded polymeric micelles (DPc/m) without irradiation (*filled square*) and with 10 min irradiation at a fluence of 1.8 J/cm2 (*unfilled square*). **A** 24 h incubation after photoirradiation; **B** 48 h incubation after photoirradiation. Data are shown as mean ± SD (n=4).

In this study, we successfully achieved the light-induced activation of chemotherapeutic agents by the PCI using the combination of CPT/m and DPc/m under the condition at which the photosensitizer (PS) alone showed no photocytotoxicity. Although there are several previous reports regarding the photo-activated chemotherapy using the combination of chemotherapeutic agents and PSs, in those studies the light-induced enhancement of the cytotoxicity of chemotherapeutic agents was observed only when the PS alone showed significant photocytotoxicity (42,43). The highly light-selective activation of chemotherapeutic agents by our system may be attributed to (1) the aforementioned CPT release selectively after the endosomal escape of CPT/m by the PCI and (2) highly selective photodamage to the endo-/lysosomal compartments by DPc/m. It is reported that low-molecular weight PSs such as sulfonated phthalocyanine ($AlPcS_{2a}$), which were used in other studies, show significant photocytotoxicity accompanied by the PCI (8,9), probably because they are assumed to accumulate not only in the endo-/lysosomes but also in other organelles susceptible to the photodamage such as the plasma membranes and mitochondria. In contrast, DPc/m is assumed to accumulate selectively in the endo-/lysosomes, thereby achieving the PCI without compromising the cytotoxicity. Regarding the intracellular behaviors of DPc/m upon photoirradiation, we previously reported that DPc/m showed 100-fold higher *in vitro* photocytotoxicity against HeLa cells than free DPc, which cannot be explained by four times higher cellular uptake of DPc/m compared with free DPc (24). Therefore, it appears that DPc/m in a micellar form should play a pivotal role in the intracellular photochemical reactions rather than released free DPc. Indeed, we confirmed that the physicochemical

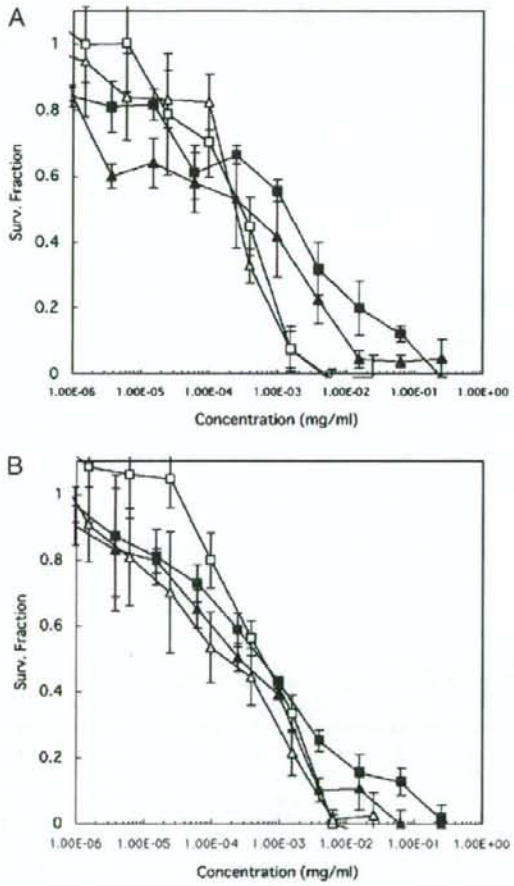

Fig. 8. Cell viability after treatment with CPT and CPT-DP combined with a non-toxic concentration of DPc/m with and without 10 min irradiation at a fluence of 1.8 J/cm^2. **A** 24 h incubation after photoirradiation; **B** 48 h incubation after photoirradiation. Non-photoirradiated CPT plus DPc/m, *filled square*; non-photoirradiated CPT-DP plus DPc/m, *filled triangle*; photoirradiated CPT plus DPc/m, *unfilled square*; photoirradiated CPT-DP plus DPc/m, *unfilled triangle*. Data are shown as mean ± SD (n=4).

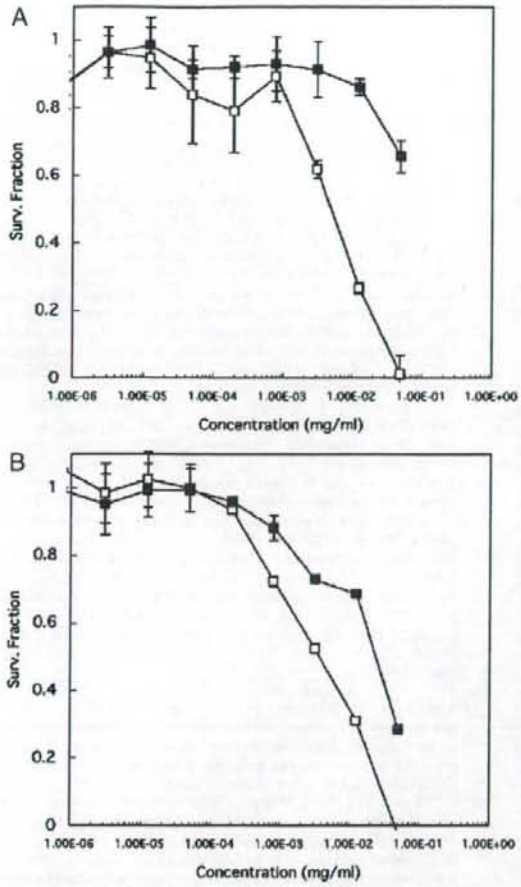

Fig. 9. Cell viability for CPT/m combined with a non-toxic concentration of DPc/m with and without 10 min irradiation at a fluence of 1.8 J/cm^2. **A** 24 h incubation after photoirradiation; **B** 48 h incubation after photoirradiation. Non-photoirradiated CPT-DP plus DPc/m, *filled square*; photoirradiated CPT/m plus DPc/m, *unfilled square*. Data are shown as mean ± SD (n=4).

properties (scattering light intensity, cumulant diameter and polydispersity index) of DPc/m were not changed during the photoirradation under the tested conditions in this study (Supporting Information). The detailed intracellular behaviors of DPc/m are now under investigation, and the results will be reported elsewhere in the near future.

Recent developments in fiber optics and laser technology allow illuminating many sites inside the human body, e.g. gastrointestinal tract, urogenital organs, lungs, brain and pancreas. However, as for PDT, one important *in vivo* restriction is the limited penetration of light into the tissue. In tissues, the light penetration decays approximately exponentially (e^{-1}) for every 2–3 mm, with a theoretical maximum for PDT effects of about 1 cm if a photosensitizer that absorbs in the far-red region of the light spectrum is used (9). For PCI, the penetration depth would be substantially larger, since very good PCI effects can be achieved with very feeble light doses. Accordingly, the penetration depths of light for effective PCI could be expected at approximately 2 cm (9). In addition, in the PCI-mediated chemotherapy, chemotherapeutic agents released from the nanocarriers after photoirradiation can diffuse through the tumor tissue, allowing the treatment of thicker and hypoxic tumors, which are known to be intractable by PDT alone due to the limited light penetration and low oxygen concentration, respectively. Another benefit of PDT and chemotherapy combination is that PDT has shown to overcome multidrug resistance in many *in vivo* tumor models (43). Recent *in vitro* results indicated that PCI has the ability to circumvent the multidrug resistance in adriamycin-resistant breast cancer MCF-7 cells by release of the adriamycin localized at end-/lysosomes after PCI (42, 44, 45).

CONCLUSION

We have designed a novel PCI-activated drug carrier for the delivery of CPT using the glutathione-sensitive polymeric micelle. The micelle showed very low release of free drug under physiological conditions. However, in the presence of a reductive agent (DTT), the drug release increased rapidly. The effect of PCI strikingly enhances the *in vitro* cytotoxicity of CPT/m by augmenting the micelle access to the cytosol. The PCI employing the combinational micelle formulations of DPc/m and CPT/m could allow the long-sought ability to deliver chemotherapeutics where, when, and in the required doses, thus maximizing their effect and reducing side effects and damage to healthy tissues. The present results not only

Table I. *In Vitro* Cytotoxicity of Free Camptothecin, Thiolated Camptothecin, CPT-Loaded Micelles Plus 1×10^{-4} mg/ml of Dendrimer Phthalocyanine-loaded Micelles Against HeLa Cells

		IC50 (μM)[a]		
Irradiation (min)	Post-incubation (h)	CPT + DPc/m	CPT-DP + DPc/m	CPT/m + DPc/m
0	24	2	1	N.D.
0	48	1.5	0.4	65
10[b]	24	1	0.7	20
10	48	1.5	0.2	10

CPT Camptothecin, *CPT-DP* thiolated camptothecin, *CPT/m* CPT-loaded micelles, *DPc/m* dendrimer phthalocyanine-loaded micelles
[a] IC50 value obtained by 3-(4,5-dimethylthiazol-2yl)-2,5-diphenyltetrazolium bromide assay
[b] Cells were photoirradiated at a fluence of 1.8 J/cm^2

warrant the further development of CPT/m with respect to the optimization and the *in vivo* development, but also indicate the potential of the PCI technology applied to polymeric micelles that specifically release their contents under reductive conditions.

ACKNOWLEDGEMENT

This research was supported in part by the New Energy and Industrial Technology Development Organization of Japan (project code: P06042), Grant-in-Aid for Cancer Research from the Ministry of Education, Culture, Sports, Science and Technology as well as Grant-in-Aid for Cancer Research and Nanomedicine projects from Ministry of Health, labour and Welfare, Japan.

REFERENCES

1. N. K. Mal, M. Fujiwara, and Y. Tanaka. Photocontrolled reversible release of guest molecules from coumarin modified mesoporous silica. *Nature* **421**:350–353 (2003). doi:10.1038/nature01362.
2. A. Mueller, B. Bondurant, and D.F. O'Brien. Visible-light-stimulated destabilization of PEG-liposomes. *Macromolecules* **33**:4799–4804 (2000). doi:10.1021/ma000055l.
3. B. Bondurant, A. Mueller, and D. F. O'Brien. Photoinitiated destabilization of sterically stabilized liposomes. *Biochim. Biophys. Acta.* **1511**:113–122 (2001). doi:10.1016/S0005-2736(00)00388-6.
4. J. Lu, E. Choi, F. Tamanoi, and J. I. Zink. Light-activated nanoimpeller-controlled drug release in cancer cells. *Small* **4**:421–426 (2008). doi:10.1002/smll.200700903.
5. C. P. McCoy, C. Rooney, C. R. Edwards, D. S. Jones, and S. P. Gorman. Light-triggered molecule-scale drug dosing devices. *J. Am. Chem. Soc.* **129**:9572–9573 (2007). doi:10.1021/ja073053q.
6. K. Berg, P. K. Selbo, L. Prasmickaite, T. E. Tjelle, K. Sandvig, J. Moan, G. Gaudernack, Ø. Fodstad, S. Kjølsrud, H. Anholt, G. H. Rodal, S. K. Rodal, and A. Høgset. Photochemical internalization: a novel technology for delivery of macromolecules into cytosol. *Cancer Res.* **59**:1180–1183 (1999).
7. P. K. Selbo, K. Sandvig, V. Kirveliene, and K. Berg. Release of gelonin from endosomes and lysosomes to cytosol by photochemical internalization. *Biochim. Biophys. Acta.* **1475**:307–313 (2000).
8. A. Høgset, L. Prasmickaite, T. E. Tjelle, and K. Berg. Photochemical transfection: a new technology for light-induced, site-directed gene delivery. *Hum. Gene Ther.* **11**:869–880 (2000). doi:10.1089/10430340050015482.
9. A. Høgset, L. Prasmickaite, P. K. Selbo, M. Hellum, B. Ø. Engesæter, A. Bonsted, and K. Berg. Photochemical internalisation in drug and gene delivery. *Adv. Drug Deliv. Rev.* **56**:95–115 (2004). doi:10.1016/j.addr.2003.08.016.
10. N. Nishiyama, A. Iriyama, W-D. Jang, K. Miyata, K. Itaka, Y. Inoue, H. Takahashi, Y. Yanagi, Y. Tamaki, H. Koyama, and K. Kataoka. Light-induced gene transfer from packaged DNA enveloped in a dendrimeric photosensitizer. *Nat. Mater.* **4**:934–941 (2005). doi:10.1038/nmat1524.
11. N. Nishiyama, Arnida, W-D. Jang, K. Date, K. Miyata, and K. Kataoka. Photochemical enhancement of transgene expression by polymeric micelles incorporating plasmid DNA and dendrimer-based photosensitizer. *J. Drug Targeting* **14**:413–424 (2006). doi:10.1080/10611860600834508.
12. Arnida, N. Nishiyama, W-D. Jang, Y. Yamasaki, and K. Kataoka. Novel ternary polyplex of triblock copolymer, pDNA and anionic dendrimer phthalocyanine for photochemical enhancement of transgene expression. *J. Control. Release* **116**:e75–e77 (2006). doi:10.1016/j.jconrel.2006.09.058.
13. Arnida, N. Nishiyama, N. Kanayama, W-D. Jang, Y. Yamasaki, and K. Kataoka. PEGylated gene nanocarriers based on block catiomers bearing ethylenediamine repeating units directed to remarkable enhancement of photochemical transfection. *J. Control. Release* **115**:208–215 (2006).
14. K. R. Weishaupt, C. J. Gomer, and T. J. Dougherty. Identification of singlet oxygen as the cytotoxic agent in photoinactivation of a murine tumor. *Cancer Res.* **36**:2326–2329 (1976).
15. H. I. Pass. Photodynamic therapy in oncology: mechanisms and clinical use. *J. Natl. Cancer Inst.* **85**:443–456 (1993). doi:10.1093/jnci/85.6.443.
16. S. B. Brown, E. A. Brown, and I. Walker. The present and future role of photodynamic therapy in cancer treatment. *Lancet Oncol.* **5**:497–508 (2004). doi:10.1016/S1470-2045(04)01529-3.
17. A. Meister, and M. E. Anderson. Glutathione. *Annu. Rev. Biochem.* **52**:711–760 (1983). doi:10.1146/annurev.bi.52.070183.003431.
18. K. Kataoka, A. Harada, and Y. Nagasaki. Block copolymer micelles for drug delivery: design, characterization and biological significance. *Adv. Drug Deliv. Rev.* **47**:113–131 (2001). doi:10.1016/S0169-409X(00)00124-1.
19. R. Duncan. The dawning era of polymer therapeutics. *Nature Rev. Drug Discov.* **2**:347–360 (2003). doi:10.1038/nrd1088.
20. N. Nishiyama, and K. Kataoka. Current sate, achievements, and future prospects of polymeric micells as nanocarriers for drug and gene delivery. *Pharmacol. & Ther.* **112**:630–648 (2006). doi:10.1016/j.pharmthera.2006.05.006.
21. A. Lavasanifar, J. Samuel, and G. S. Kwon. Poly(ethylene oxide)-block-poly(L-amino acid) micelles for drug delivery. *Adv. Drug Deliv. Rev.* **54**:169–190 (2002). doi:10.1016/S0169-409X(02)00015-7.
22. Y. Matsumura, and H. Maeda. A new concept for macromolecular therapeutics in cancer chemotherapy: mechanism of tumoritropic accumulation of proteins and the antitumor agent SMANCS. *Cancer Res.* **46**:6387–6392 (1986).
23. W-D. Jang, N. Nishiyama, G-D Zhang, A. Harada, D-L Jiang, S. Kawauchi, Y. Morimoto, M. Kikuchi, H. Koyama, T. Aida, and K. Kataoka. Supramolecular nanocarrier of anionic dendrimer porphyrins with cationic block copolymers modified with poly (ethylene glycol) to enhance intracellular photodynamic efficacy. *Angew. Chemie., Int. Ed.* **117**:423–427 (2005). doi:10.1002/ange.200461603.
24. W-D. Jang, Y. Nakagishi, N. Nishiyama, S. Kawauchi, Y. Morimoto, M. Kikuchi, and K. Kataoka. Polyion complex micelles for photodynamic therapy: Incorporation of dendritic photosensitizer excitable at long wavelength relevant to improved tissue-penetrating property. *J Control. Release* **113**:73–79 (2006). doi:10.1016/j.jconrel.2006.03.009.
25. J. O'Leary, and F. M. Muggia. Camptothecins: a review of their development and schedules of administration. *Eur. J. Cancer* **34**:1500–1508 (1998). doi:10.1016/S0959-8049(98)00229-9.
26. B. C. Giovanella, N. Harris, J. Mendoza, Z. Cao, J. Liehr, and J. S. Stehlin. Dependence of anticancer activity of camptothecins on maintaining their lactone function. *Ann. New York Acad. Sci.* **922**:27–35 (2000).
27. N. Nishiyama, S. Okazaki, H. Cabral, M. Miyamoto, Y. Kato, Y. Sugiyama, K. Nishio, Y. Matsumura, and K. Kataoka. Novel cisplatin-incorporated polymeric micelles can eradicate solid tumors in mice. *Cancer Res.* **63**:8977–8983 (2003).
28. A. C. H. Ng, X. Li, and D. K. P. Ng. Synthesis and photophysical properties of nonaggregated phthalocyanines bearing dendritic substitutes. *Macromolecules* **32**:5292–5298 (1999). doi:10.1021/ma990367s.
29. A. Harada, and K. Kataoka. Formation of polyion complex micelles in an aqueous milieu form a pair of oppositely charged block copolymers with poly(ethylene glycol) segments. *Macromolecules* **28**:5294–5299 (1995). doi:10.1021/ma00119a019.
30. Y. Kakizawa, A. Harada, and K. Kataoka. Environment-sensitive stabilization of core-Shell structured polyion complex micelle by reversible cross-Linking of the core through disulfide bond. *J. Am. Chem. Soc.* **121**:11247–11248 (1999). doi:10.1021/ja993057y.
31. K. Miyata, Y. Kakizawa, N. Nishiyama, A. Harada, Y. Yamasaki, H. Koyama, and K. Kataoka. Block catiomer polyplexes with regulated densities of charge and disulfide cross-linking directed to enhance gene expression. *J. Am. Chem. Soc.* **126**:2355–2361 (2004). doi:10.1021/ja0379666.
32. K. Miyata, Y. Kakizawa, N. Nishiyama, Y. Yamasaki, T. Watanabe, M. Kohara, and K. Kataoka. Practically applicable cross-linked polyplex micelle with high tolerability against freeze-drying for *in vivo* gene delivery. *J. Control. Release.* **109**:15–23 (2005). doi:10.1016/j.jconrel.2005.09.043.

33. K. Berg, A. Dietze, O. Kaalhus, and A. Høgset. Site-specific drug delivery by photochemical internalization enhances the antitumor effect of Bleomycin. *Clin. Cancer Res.* **11**:8476–8485 (2005). doi:10.1158/1078-0432.CCR-05-1245.
34. R. Greenwald, A. Pendri, C. Conover, C. Gilbert, R. Yang, and J. Xia. Drug delivery systems. 2. Camptothecin-20-O- poly (ethylene glycol) ester transport forms. *J. Med. Chem.* **39**:1938–1940 (1996). doi:10.1021/jm9600555.
35. B. B. Lundberg. Biologically active camptothecin derivatives for incorporation into liposome bilayers and lipid emulsions. *Anticancer Drug Design.* **13**:453–461 (1998).
36. X. Liu, B. C. Lynn, J. Zhang, L. Song, D. Bom, W. Du, D.P. Curran, and T. G. Burke. A versatile prodrug approach for liposomal core-loading of water-insoluble camptothecin anticancer drugs. *J. Am. Chem. Soc.* **124**:7650–7661 (2002). doi:10.1021/ja0256212.
37. A. Shenderova, T. G. Burke, and S. P. Schwendeman. Stabilization of 10-hydroxycamptothecin in poly(lactide-co-glycolide) microsphere delivery vehicles. *Pharm. Res.* **14**:1406–1414 (1997). doi:10.1023/A:1012172722246.
38. B. Ertl, and P. Platzer. Poly(D,L-lactide-co-glycolide) microspheres for sustained delivery and stabilization of camptothecin. *J. Control. Release* **61**:305–317 (1999). doi:10.1016/S0168-3659(99)00122-4.
39. K. M. Tyner, S. R. Schiffman, and E. P. Giannelis. Nanobiohybrids as delivery vehicles for camptothecin. *J. Control. Rel.* **95**:501–514 (2004). doi:10.1016/j.jconrel.2003.12.027.
40. P. Opanasopit, M. Yokoyama, M. Watanabe, K. Kawano, Y. Maitani, and T. Okano. Block copolymer design for camptothecin incorporation into polymeric micelles for passive tumor targeting. *Pharm. Res.* **21**:2001–2008 (2004). doi:10.1023/B:PHAM.0000048190.53439.eb.
41. R. Barreiro-Iglesias, L. Bromberg, M. Temchenko, T. A. Hatton, A. Concheiro, and C. Alvarez-Lorenzo. Solubilization and stabilization of camptothecin in micellar solutions of pluronic-g-poly(acrylic acid) copolymers. *J. Control. Release.* **97**:537–549 (2004).
42. P-J. Lou, P-S. Lai, M-J Shieh, A. J. MacRobert, K. Berg, and S. G. Bown. Reversal of doxorubicin resistance in breast cancer cells by photochemical internalization. *Int. J. Cancer* **119**:2692–2698 (2006). doi:10.1002/ijc.22098.
43. P. S. Lai, P. J. Lou, C. L. Peng, C. L. Pai, W. N. Yen, M. Y. Huang, T. H. Young, and M. J. Shieh. Doxorubicin delivery by polyamidoamine dendrimer conjugation and photochemical internalization for cancer therapy. *J. Control. Release* **122**:39–36 (2007). doi:10.1016/j.jconrel.2007.06.012.
44. M. A. M Capella, and L. S. Capella. A light in multidrug resistance: photodynamic treatment of multidrug-resistant tumors. *J. Biomed. Sci.* **10**:361–366 (2003). doi:10.1007/BF02256427.
45. D. K. Adigbli, D. G. G. Wilson, N. Farooqui, E. Sousi, P. Risley, I. Taylor, A. J. MacRobert, and M. Loizidou. Photochemical internalisation of chemotherapy potentiates killing of multidrug-resistant breast and bladder cancer cells. *Br. J. Cancer* **97**:502–512 (2007). doi:10.1038/sj.bjc.6603895.

molecular pharmaceutics

Subscriber access provided by UNIV OF TOKYO

Article

Polyplex Micelles with Cyclic RGD Peptide Ligands and Disulfide Cross-Links Directing to the Enhanced Transfection via Controlled Intracellular Trafficking

Makoto Oba, Kazuhiro Aoyagi, Kanjiro Miyata, Yu Matsumoto, Keiji Itaka, Nobuhiro Nishiyama, Yuichi Yamasaki, Hiroyuki Koyama, and Kazunori Kataoka

Mol. Pharmaceutics, **2008**, 5 (6), 1080-1092 • DOI: 10.1021/mp800070s • Publication Date (Web): 08 October 2008

Downloaded from http://pubs.acs.org on January 9, 2009

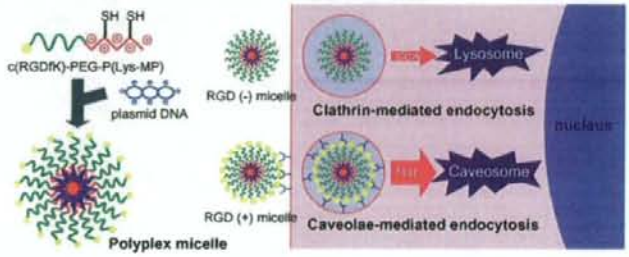

More About This Article

Additional resources and features associated with this article are available within the HTML version:

- Supporting Information
- Access to high resolution figures
- Links to articles and content related to this article
- Copyright permission to reproduce figures and/or text from this article

View the Full Text HTML

ACS Publications
High quality. High impact.

Molecular Pharmaceutics is published by the American Chemical Society. 1155 Sixteenth Street N.W., Washington, DC 20036

articles

molecular pharmaceutics

Polyplex Micelles with Cyclic RGD Peptide Ligands and Disulfide Cross-Links Directing to the Enhanced Transfection via Controlled Intracellular Trafficking

Makoto Oba,[†] Kazuhiro Aoyagi,[‡] Kanjiro Miyata,[§,∥] Yu Matsumoto,[⊥] Keiji Itaka,[⊥] Nobuhiro Nishiyama,[∥,⊥] Yuichi Yamasaki,[‡,∥] Hiroyuki Koyama,[†] and Kazunori Kataoka*[,‡,∥,⊥]

Department of Clinical Vascular Regeneration, Graduate School of Medicine, The University of Tokyo, 7-3-1 Hongo, Bunkyo, Tokyo 113-8655, Japan, Department of Materials Engineering, Graduate School of Engineering, The University of Tokyo, 7-3-1 Hongo, Bunkyo, Tokyo 113-8656, Japan, Center for NanoBio Integration, The University of Tokyo, 7-3-1 Hongo, Bunkyo, Tokyo 113-8656, Japan, Department of Bioengineering, Graduate School of Engineering, The University of Tokyo, 7-3-1 Hongo, Bunkyo, Tokyo 113-8656, Japan, and Center for Disease Biology and Integrative Medicine, Graduate School of Medicine, The University of Tokyo, 7-3-1 Hongo, Bunkyo, Tokyo 113-0033, Japan

Received June 24, 2008; Revised Manuscript Received September 16, 2008; Accepted September 23, 2008

Abstract: Thiolated c(RGDfK)-poly(ethylene glycol)-*block*-poly(lysine) (PEG-PLys), a novel block polymer that has a cyclic RGD peptide in the PEG terminus and thiol groups in the PLys side chain, was prepared and applied to the preparation of targetable disulfide cross-linked polyplex micelles through ion complexation with plasmid DNA (pDNA). The obtained polyplex micelles achieved remarkably enhanced transfection efficiency against cultured HeLa cells possessing $\alpha_v\beta_3$ integrin receptors, which are selectively recognized by cyclic RGD peptides, demonstrating the synergistic effect of cyclic RGD peptide ligands on the micelle surface and disulfide cross-links in the core to exert the smooth release of pDNA in the intracellular environment via reductive cleavage. This enhancement was not due to an increase in the uptake amount of polyplex micelles but to a change in their intracellular trafficking route. Detailed confocal laser scanning microscopic observation revealed that polyplex micelles with cyclic RGD peptide ligands were distributed in the perinuclear region in the early stages preferentially through caveolae-mediated endocytosis, which may be a desirable pathway for avoiding the lysosomal degradation of delivered genes. Hence, this approach to introducing ligands and cross-links into the polyplex micelles is promising for the construction of nonviral gene vectors that enhance transfection by controlling intracellular distribution.

Keywords: Polymeric micelle; cyclic RGD peptide; disulfide cross-links; caveolae-mediated endocytosis

Introduction

As an alternative to viral gene vectors with intrinsic safety issues, there is a growing demand for nonviral gene vectors.[1,2] Despite this demand, nonviral gene vectors based on cationic lipids (lipoplexes) and cationic polymers (polyplexes) are still insufficiently for *in vivo* applications, particularly those administered systemically. To achieve

* To whom correspondence should be addressed. Mailing address: The University of Tokyo, Department of Materials Engineering, 7-3-1 Hongo, Bunkyo-ku, Tokyo, 113-8656, Japan. Tel: +81-3-5841-7138. Fax: +81-3-5841-7139. E-mail: kataoka@bmw.t.u-tokyo.ac.jp.

† Department of Clinical Vascular Regeneration, Graduate School of Medicine.

‡ Department of Materials Engineering, Graduate School of Engineering.

§ Department of Bioengineering, Graduate School of Engineering.

∥ Center for NanoBio Integration.

⊥ Center for Disease Biology and Integrative Medicine, Graduate School of Medicine.

10.1021/mp800070s CCC: $40.75 © 2008 American Chemical Society
Published on Web 10/08/2008

sufficient *in vivo* systemic transfection, nonviral vectors need to satisfy several properties, such as high stability in the bloodstream, accumulation in target tissues, and controlled intracellular trafficking directing to the nucleus.

Polyplex micelles, composed of poly(ethylene glycol) (PEG)-polycation block copolymers and plasmid DNA (pDNA), are nonviral gene vectors with the potential for systemic application,[3−5] because of the suitable size of approximately 100 nm for systemic administration, and the formation of the biocompatible PEG shell layer to avoid the nonspecific interaction with blood components.[6−8] To further improve the stability and transfection efficiency of polyplex micelles, disulfide cross-links were introduced into the micelle core, revealing the improved transfection to cultured cells as well as the successful reporter gene expression in mouse liver by systemic administration.[9,10] Furthermore, we recently established a procedure to install cyclic RGD peptide ligands (c(RGDfK)), which can selectively recognize $\alpha_v\beta_3$ and $\alpha_v\beta_5$ integrin receptors, on the surface of a polyplex micelle. Eventually, c(RGDfK) installed polyplex micelles exhibited enhanced transfection efficiency against specific cells possessing $\alpha_v\beta_3$ and $\alpha_v\beta_5$ integrin receptors, such as HeLa cells.[11] $\alpha_v\beta_3$ integrin receptors are known to be overexpressed in endothelial cells of tumor capillaries and neointimal tissues. It should be noted that the use of vectors with cyclic RGD peptide ligands has been investigated as an active targeting strategy in antiangiogenic gene therapy for cancer.[12−14] Nevertheless, those studies focused primarily on therapeutic through the facilitation of cellular uptake of the vectors through receptor-mediated routes, and less attention has been paid to the intracellular trafficking of the vectors possibly modulated by the installed ligands. Worth mentioning in this regard is our previous finding that installation of cyclic RGD ligands on the polyplex micelle surface facilitated their localization in the perinuclear region, suggesting the modulated trafficking induced by cyclic RGD ligands.[11]

The study reported here is devoted to get further insights into the modulated cellular uptake and subsequent trafficking of c(RGDfK) installed polyplex micelles in order to enhance transfection efficiency. For this purpose, new polyplex micelles with integrated functions were developed by installing cyclic RGD ligands on the surface and disulfide cross-links in the core. Indeed, the PEG-*block*-poly(lysine) (PEG-PLys) block copolymer as a platform polymer was modified by introducing a cyclic RGD peptide into the PEG terminus as well as thiol groups into the side chain of the PLys segment. The functions of prepared polyplex micelles were tested against HeLa cells possessing $\alpha_v\beta_3$ and $\alpha_v\beta_5$ integrin receptors; the transfection efficiency, the amount of cellular uptake, and the intracellular distribution were thus determined. In particular, the intracellular trafficking of the polyplex micelles loaded with Cy3- or Cy5-labeled pDNA was evaluated thoroughly by confocal laser scanning microscope (CLSM) observation, which clarified the uptake route and the final intracellular localization. The results demonstrated that cyclic RGD ligands facilitated the caveolae-mediated endocytosis of the polyplex micelles and thus improved transfection efficiency, which is apparently important for the design of nonviral gene vectors that can avoid lysosomal degradation. Moreover, cyclic RGD ligands should

(1) Pack, D. W.; Hoffman, A. S.; Pun, S.; Stayton, P. S. Design and Development of Polymers for Gene Delivery. *Nat. Rev. Drug Discovery* **2005**, *4*, 581–593.

(2) Mastrobattista, E.; van der Aa, M. A.; Hennink, W. E.; Crommelin, D. J. A. Artificial Viruses: a Nanotechnological Approach to Gene Delivery. *Nat. Rev. Drug Discovery* **2006**, *5*, 115–121.

(3) Katayose, S.; Kataoka, K. Water-Soluble Polyion Complex Associates of DNA and Poly(ethylene glycol)-Poly(L-lysine) Block Copolymer. *Bioconjugate Chem.* **1997**, *8*, 702–707.

(4) Kakizawa, Y.; Kataoka, K. Block Copolymer Micelles for Delivery of Gene and Related Compounds. *Adv. Drug Delivery Rev.* **2002**, *54*, 203–222.

(5) Osada, K.; Kataoka, K. Drug and Gene Delivery Based on Supramolecular Assembly of PEG-Polypeptide Hybrid Block Copolymers. *Adv. Polym. Sci.* **2006**, *202*, 113–153.

(6) Itaka, K.; Yamauchi, K.; Harada, A.; Nakamura, K.; Kawaguchi, H.; Kataoka, K. Polyion Complex Micelles from Plasmid DNA and Poly(ethylene glycol)-Poly(L-lysine) Block Copolymer as Serum-Tolerable Polyplex System: Physicochemical Properties of Micelles Relevant to Gene Transfection Efficiency. *Biomaterials* **2003**, *24*, 4495–4506.

(7) Han, M.; Bae, Y.; Nishiyama, N.; Miyata, K.; Oba, M.; Kataoka, K. Transfection Study Using Multicellular Tumor Spheroids for Screening Non-Viral Polymeric Gene Vectors with Low Cytotoxicity and High Transfection Efficiencies. *J. Controlled Release* **2007**, *121*, 38–48.

(8) Akagi, D.; Oba, M.; Koyama, H.; Nishiyama, N.; Fukushima, S.; Miyata, T.; Nagawa, H.; Kataoka, K. Biocompatible Micellar Nanovectors Achieve Efficient Gene Transfer to Vascular Lesions without Cytotoxicity and Thrombus Formation. *Gene Ther.* **2007**, *14*, 1029–1038.

(9) Miyata, K.; Kakizawa, Y.; Nishiyama, N.; Harada, A.; Yamasaki, Y.; Koyama, H.; Kataoka, K. Block Catiomer Polyplexes with Regulated Densities of Charge and Disulfide Cross-Linking Directed to Enhanced Gene Expression. *J. Am. Chem. Soc.* **2004**, *126*, 2355–2361.

(10) Miyata, K.; Kakizawa, Y.; Nishiyama, N.; Yamasaki, Y.; Watanabe, T.; Kohara, M.; Kataoka, K. Freeze-Dried Formulations for In Vivo Gene Delivery of PEGylated Polyplex Micelles with Disulfide Crosslinked Cores to the Liver. *J. Controlled Release* **2005**, *109*, 15–23.

(11) Oba, M.; Fukushima, S.; Kanayama, N.; Aoyagi, K.; Nishiyama, N.; Koyama, H.; Kataoka, K. Cyclic RGD Peptide-Conjugated Polyplex Micelles as a Targetable Gene Delivery System Directed to Cells Possessing $\alpha_v\beta_3$ and $\alpha_v\beta_5$ Integrins. *Bioconjugate Chem.* **2007**, *18*, 1415–1423.

(12) Kim, W. J.; Yockman, J. W.; Lee, M.; Jeong, J. H.; Kim, Y. H.; Kim, S. W. Soluble *Flt-1* Gene Delivery Using PEI-*g*-PEG-RGD Conjugate for Anti-Angiogenesis. *J. Controlled Release* **2005**, *106*, 224–234.

(13) Kim, W. J.; Yockman, J. W.; Jeong, J. H.; Christensen, L. V.; Lee, M.; Kim, Y. H.; Kim, S. W. Anti-Angiogenic Inhibition of Tumor Growth by Systemic Delivery of PEI-*g*-PEG-RGD/pCMV-sFlt-1 Complexes in Tumor-Bearing Mice. *J. Controlled Release* **2006**, *114*, 381–388.

(14) Schiffelers, R. M.; Ansari, A.; Xu, J.; Zhou, Q.; Tang, Q.; Storm, G.; Molema, G.; Lu, P. Y.; Scaria, P. V.; Woodle, M. C. Cancer siRNA Therapy by Tumor Selective Delivery with Ligand-Targeted Sterically Stabilized Nanoparticle. *Nucleic Acids Res.* **2004**, *32*, e149.

eventually achieve appreciable transfection efficiency even for systems without high endosomal-disrupting properties, including PLys-based polyplex systems.

Experimental Section

Materials. *N,N*-Diisopropylethylamine (DIEA), dithiothreitol (DTT), aphidicolin, and D-luciferin were purchased from Wako Pure Chemical Industries (Osaka, Japan). *N*-Methyl-2-pyrrolidone (NMP) was purchased from Aldrich Chemical (Milwaukee, WI). *N*-Succinimidyl 3-(2-pyridyldithio)-propionate (SPDP) was purchased from Dojindo Laboratories (Kumamoto, Japan). Cyclo[RGDfK(CX-)] (c(RGDfK)) peptides (X = 6-aminocaproic acid: ε-Acp) was purchased from Peptide Institute (Osaka, Japan). Acetal-poly(ethylene glycol)-*block*-poly(lysine) (acetal-PEG-PLys) and c(RGDfK)-PEG-PLys block copolymers (PEG, 12 000 g/mol; polymerization degree of PLys segment, 72; introduction rate of c(RGDfK) peptide, 66%) were synthesized as previously reported.[11] A micro-BCA protein assay reagent kit was purchased from Pierce Chemical (Rockford, IL). The luciferase assay kit was a product of Promega (Madison, WI). Plasmid pCAcc+Luc coding for firefly luciferase under the control of the CAG promoter was provided by RIKEN Gene Bank (Tsukuba, Japan), amplified in competent DH5α *Escherichia coli*, and then purified using a HiSpeed Plasmid MaxiKit purchased from Qiagen Sciences (Germantown, MD).

Synthesis of Block Copolymers: (a) Acetal-poly(ethylene glycol)-block-poly[ε-3-(2-pyridyldithio)propionyl lysine] (Acetal-PEG-P(Lys-PDP)). Pyridyldithiopropionyl (PDP) groups were introduced to the PLys side chain by the use of a heterobifunctional reagent, SPDP. The typical synthesis procedure is described as follows for the acetal-PEG-P(Lys-PDP) (5 mol % PDP): Acetal-PEG-PLys (200 mg, 8.38 μmol) and SPDP (11.7 mg, 37.7 μmol) were separately dissolved in NMP containing 5 wt % LiCl (10 mL for acetal-PEG-PLys, 1 mL for SPDP). A solution containing SPDP and DIEA (1.05 mL, 377 μmol) was added to acetal-PEG-PLys solution and stirred at room temperature for 3 h. The mixture was then precipitated into an approximately 20-times-excess volume of diethyl ether. The polymer was dissolved in 10 mM phosphate buffer (pH 7.0) with 150 mM NaCl, dialyzed against the same buffer solution and distilled water, and lyophilized to obtain acetal-PEG-P(Lys-PDP) (166 mg, 80%).

(b) c(RGDfK)-poly(ethylene glycol)-block-poly[ε-(3-mercaptopropinonyl) lysine] (c(RGDfK)-PEG-P(Lys-MP)). The typical synthesis procedure is described as follows for the c(RGDfK)-PEG-P(Lys-MP) (5 mol % MP): Acetal-PEG-P(Lys-PDP) (30 mg, 1.21 μmol) was dissolved in 10 mM Tris-HCl buffer solution (pH 7.4) (3 mL) with DTT (6.76 mg, 43.9 μmol). After 30 min incubation at room temperature, the polymer solution was dialyzed against 0.2 M AcOH buffer (pH 4.0). c[RGDfK(CX-)] (10.4 mg, 12.8 mmol) in AcOH buffer (3 mL) was then added to the polymer solution. After stirring for 5 days, DTT (6.67 mg, 43.9 μmol) was added and stirred at room temperature for 3 h. The reacted polymer was purified by dialysis sequentially against 10 mM phosphate buffer (pH 7.0) with 150 mM NaCl and distilled water, and lyophilized to obtain c(RGDfK)-PEG-P(Lys-MP) (20.5 mg, 71%).

The ^{1}H NMR spectrum of each polymer was obtained with an EX300 spectrometer (JEOL, Tokyo, Japan). Chemical shifts were reported in ppm relative to the residual protonated solvent resonance. Block copolymer with X% of thiolation degree was abbreviated as B-SHX%.

Preparation of Polyplex Micelles. Each thiolated block copolymer was dissolved in 10 mM Tris-HCl buffer (pH 7.4), followed by the addition of 3-times-excess mol of DTT against the PDP or MP group. After 30 min incubation at room temperature, the polymer solution in varying concentrations was added to a twice-excess volume of 50 μg/mL pDNA/10 mM Tris-HCl (pH 7.4) solution to form polyplex micelles with different compositions. The final pDNA concentration was adjusted to 33.3 μg/mL. The N/P ratio was defined as the residual molar ratio of amino groups of PLys to the phosphate groups of pDNA. After overnight incubation at room temperature, the polyplex micelle solution was dialyzed against 10 mM Tris-HCl (pH 7.4) containing 0.5 vol% DMSO at 37 °C for 24 h to remove the impurities, followed by 2 days of additional dialysis to remove DMSO. During the dialysis, the thiol groups of thiolated block copolymers were oxidized to form disulfide cross-links. To follow the oxidation process, the remaining thiol groups in disulfide cross-linked micelles were determined by Ellman's method.[15] Polyplex micelles with and without cyclic RGD peptide ligands were abbreviated as RGD (+) and RGD (−) micelles, respectively.

Dynamic Light Scattering Measurement. The sizes of the polyplex micelles were evaluated by dynamic light scattering (DLS) using the Nano ZS zetasizer (ZEN3600, Malvern Instruments, Worcestershire, U.K.). A He−Ne ion laser (633 nm) was used for the incident beam. Polyplex micelle solutions (33.3 μg pDNA/mL) with an N/P = 2 in 10 mM Tris-HCl (pH 7.4) were used for the measurements. The data obtained at a detection angle of 173 ° and a temperature of 25 °C were analyzed by a cumulant method to obtain the hydrodynamic diameters and polydispersity indices (μ/Γ^{-2}) of the micelles. The results reported were expressed as mean values (± SEM) of four experiments.

ζ-Potential Measurement. The ζ-potentials of the polyplex micelles were evaluated by the laser-doppler electrophoresis method using Nano ZS with a He−Ne ion laser (633 nm). Polyplex micelle solution with an N/P = 2 was adjusted to a concentration of 20 μg pDNA/mL. The ζ-potential was measured at 25 °C. A scattering angle of 173 ° was used in these measurements. The results were expressed as the mean values (± SEM) of four experiments.

Atomic Force Microscopy (AFM) Imaging. Five microliters of each sample was deposited on a freshly cleaved

(15) Riddles, P. W.; Blakeley, R. L.; Zerner, B. Ellman's Reagent: 5,5′-Dithiobis(2-nitrobenzoic Acid)- a Reexamination. *Anal. Biochem.* **1979**, *94*, 75–81.

Scheme 1. Synthesis Route of c(RGDfK)-PEG-P(Lys-MP) Block Copolymer

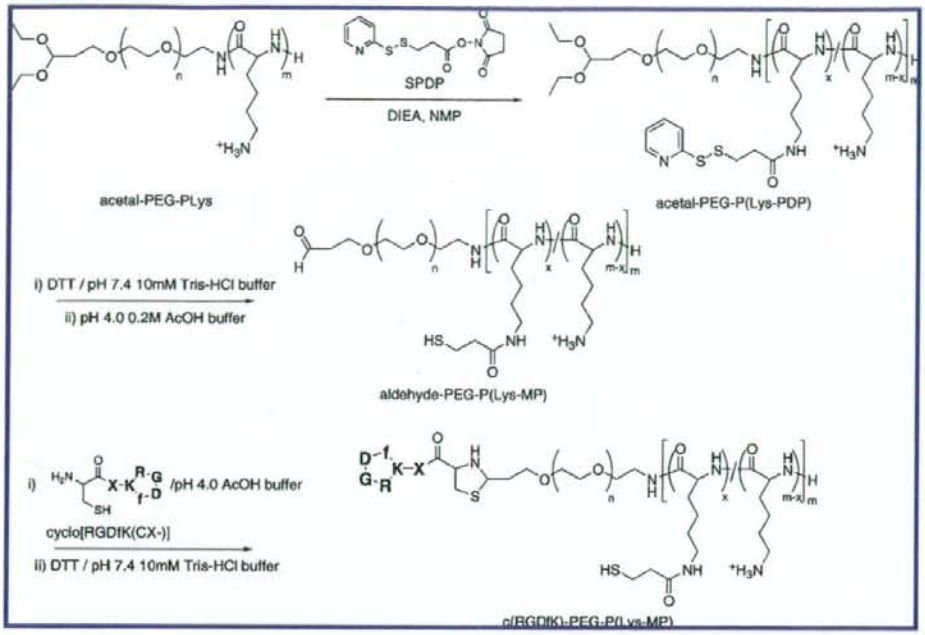

mica substrate for 30 s and then adequately dried under a gentle flow of nitrogen gas. AFM imaging was performed in a tapping mode with MPP-11100 (Vecco Instruments, Woodbury, NY) on a Nano Scope (Vecco Instruments) operated by Nanoscope IIIa software (Digital Instruments, Santa Barbara, CA). The cantilever oscillation frequency was

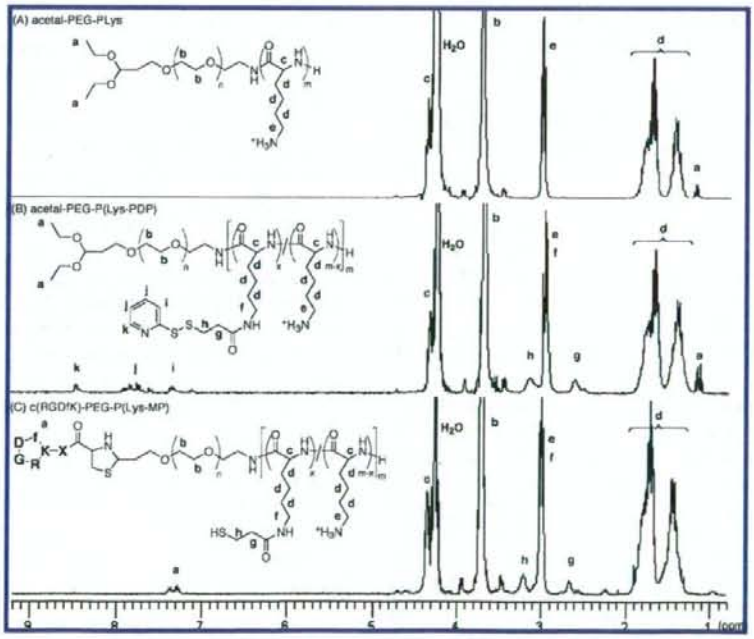

Figure 1. ^{1}H NMR spectra of acetal-PEG-PLys (A), acetal-PEG-P(Lys-PDP) (B-SH5%) (B), and c(RGDfK)-PEG-P-(Lys-MP) (B-SH5%) (C) in D_2O at 80 °C.

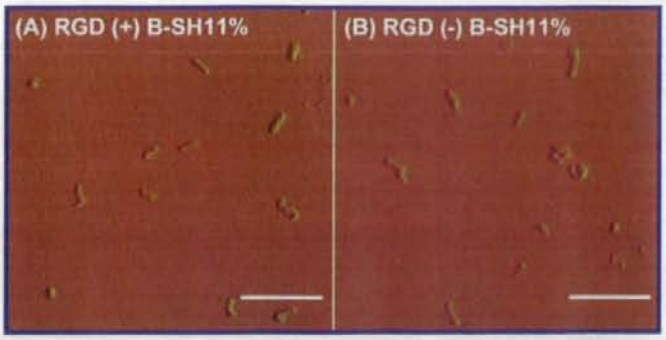

Figure 2. AFM images of cross-linked micelles (B-SH11%, N/P = 2) with (A) or without (B) cyclic RGD peptide ligands. The scale bars represent 500 nm.

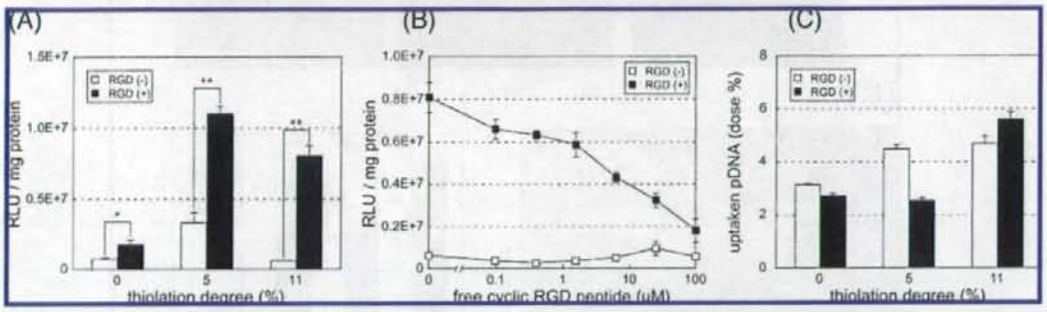

Figure 3. In vitro transfection efficiency and cellular uptake of polyplex micelles against HeLa cells. (A) Effects of cyclic RGD peptide ligands on transfection efficiency for micelles with varying thiolation degrees (N/P = 2). (B) Inhibitory effect of free cyclic RGD peptide on the transfection with B-SH11% polyplex micelles (N/P = 2) with or without cyclic RGD peptide ligands. (C) Cellular uptake of RGD (+) and RGD (−) polyplex micelles (N/P = 2) loading ^{32}P-labeled pDNA. Error bars in the graphs represent SEM, $n = 4$. $P^* < 0.05$ and $P^{**} < 0.01$.

tuned to the resonance frequency of the cantilever, 260−340 kHz. The images were recorded at a 2 μm/s linear scanning speed and with a sampling density of 61 nm^2 per pixel. Raw AFM images were processed only by background removal (flattening) using a microscope manufacturer's image-processing software.

Transfection. HeLa cells were seeded on 24-well culture plates (10 000 cells/well) and incubated overnight in 500 μL of Dulbecco's modified Eagle's medium (DMEM) containing 10% fetal bovine serum (FBS). The medium was replaced with fresh medium, after which polyplex solution (N/P = 2) was applied to each well (1 μg of pDNA/well). After 24 h incubation, the medium was replaced with 500 μL of fresh medium, followed by 24 h reincubation. The luciferase gene expression was then evaluated based on the intensity of photoluminescence intensity using the Luciferase assay kit and a Lumat LB9507 luminometer (Berthold Technologies, Bad Wildbad, Germany). The amount of protein in each well was concomitantly determined using a Micro BCA protein assay reagent kit.

Inhibitory Effect of Free Cyclic RGD Peptides. HeLa cells were seeded on 24-well culture plates (10 000 cells/well) and incubated overnight in 500 μL of DMEM containing 10% FBS. The medium was replaced with fresh medium containing various concentrations of cyclo[RGDfK(CX-)], followed by 3 h incubation. The polyplex micelle solution (B-SH11%, N/P = 2) was applied to each well (1 μg pDNA/well). After 24 h incubation, the medium was replaced with 500 μL of fresh medium, followed by 24 h reincubation. The luciferase gene expression was then evaluated in the same way as described in the Transfection section.

Analysis of Cellular Uptake of Polyplex Micelles. pDNA was radioactively labeled by incorporation of ^{32}P-dCTP (GE Healthcare U.K., Buckinghamshire, U.K.) using a nick translation system (Invitrogen, Carlsbad, CA) according to the manufacturer's protocol. Unincorporated nucleotides were carefully removed using the High Pure PCR Product Purification Kit (Roche, Basel, Switzerland). HeLa cells were seeded on 24-well culture plates (10 000 cells/well) and incubated overnight in 500 μL of DMEM containing 10% FBS. The medium was replaced with fresh medium, after which the polyplex micelle incorporating the mixture of nonlabeled and ^{32}P-labeled pDNA (N/P = 2) was applied to each well (1 μg pDNA/well). After 24 h incubation, the medium was removed and the cells were washed 3 times with PBS. The cells were lysed with 400 μL of cell culture lysis reagent (Promega) for 30 min at room temperature, after which the lysate was mixed with 5 mL of Ultima Gold